SATELLITE TRACKING ANTARCTIC MINKE WHALES (*BALAENOPTERA BONAERENSIS*) IN A DYNAMIC SEA ICE HABITAT ALONG THE WESTERN ANTARCTIC PENINSULA

by

Jessica F. Lee

A thesis submitted to the Faculty of the University of Delaware in partial fulfillment of the requirements for the degree of Master of Science in Geography

Fall 2016

SATELLITE TRACKING ANTARCTIC MINKE WHALES (*BALAENOPTERA BONAERENSIS*) IN A DYNAMIC SEA ICE HABITAT ALONG THE WESTERN ANTARCTIC PENINSULA

by

Jessica F. Lee

Approved: ______________________________
Tracy L. DeLiberty, Ph.D.
Professor in charge of thesis on behalf of Advisory Committee

Approved: ______________________________
Matthew J. Oliver, Ph.D.
Professor in charge of thesis on behalf of Advisory Committee

Approved: ______________________________
Delphis F. Levia, Jr., Ph.D.
Chair of the Department of Geography

Approved: ______________________________
Mohsen Badiey, Ph.D.
Acting Dean of the College of Earth, Ocean, and Environment

Approved: ______________________________
Ann L. Ardis, Ph.D.
Senior Vice Provost for Graduate and Professional Education

ACKNOWLEDGMENTS

I am deeply grateful for a number of individuals, who through their valuable encouragement and assistance made this thesis possible.

Firstly, I wish to thank my advisor, Dr. Tracy DeLiberty, for her unwavering support and commitment to my personal and professional growth. Tracy has been a steadfast, generous, and motivating presence in my time at UD, and I am immensely thankful and proud to be her advisee. I would also like to thank my committee members, Dr. Matthew Oliver and Dr. Ari Friedlaender. Matt and Ari provided invaluable insights and expertise in the development and implementation of this project, and I am truly grateful for their advice and dedication. Furthermore, I would like to thank Dr. Brian Hanson, Dr. Dana Veron, and the faculty in the Department of Geography, for their valuable lessons, mentorship, and inspiring passion.

Finally, I would like to extend my immense gratitude to my friends and family for their encouragement and support. I wish to express my deepest thanks to Michalea King, Kelsey Moxey, Alex Schroth, Erika Schreiber, and Renato Kane, as well as the friends I've made in and out of the department, for sharing their motivational words, academic expertise, and abiding friendship. I will cherish and miss you all as we move on to our next adventures. To my mother, father, and brothers, thanks for always being on my team and pushing me to succeed. I could not have made it this far on my academic journey without you all, thank you!

TABLE OF CONTENTS

LIST OF TABLES

LIST OF FIGURES

ABSTRACT

The Southern Ocean and Western Antarctic Peninsula (WAP) are an ecologically vital polar marine habitat supporting rich stocks of plankton, krill, and top predators. Abiotic factors such as sea ice dynamics, sea surface temperature, and bathymetry are key predictors of the spatial distribution of plankton blooms and therefore greatly affect krill and baleen whale populations. This study aims to understand the habitat preference of Antarctic minke whales (*Balaenoptera bonaerensis*) with respect to sea ice dynamics and other abiotic factors around the WAP. Ship- and aerial-based surveys have suggested this mesopredator exhibits a pagophilic nature, and we provide the first satellite tag-based habitat analysis that confirms this hypothesis. As a relatively small baleen whale species, the Antarctic minke whale is well suited to life in the pack ice where larger cetacean species are unable to maneuver or hunt as successfully. Daily movements were recorded with ARGOS satellite tags and behavioral states were described using the Multi-Scale Straightness Index. Generalized additive models (GAMs) elucidated ecological relationships between the whales and the environment. The GAMs demonstrated a strong preference for sea ice habitat, where the minke whales preferred to forage close to the sea ice edge as well as within the dense pack ice. The GAMs also indicated individual preferences with respect to sea surface temperature and bathymetry, demonstrating the importance of these variables in locating dense prey aggregations. The coupled relationship between minke whales, krill, and sea ice suggests that these whales will be sensitive to changes in sea ice concentration, extent, and duration, making them particularly vulnerable to climate change. Results from this analysis will therefore be beneficial for conservation and future research.

Chapter 1

INTRODUCTION

1.1 Antarctic Minke Whales

1.1.1 Ecology and Life History

Prior to the 1990s, only one species of minke whale was recognized, *Baleanoptera acustorostrata*, the common minke whale. In 2000, the International Whaling Commission (IWC) Scientific Committee recognized the Antarctic minke whale as a unique species, *B. bonaerensis*, while northern hemisphere minke whales and southern hemisphere dwarf minke whales are still considered *B. acustorostrata* (International Whaling Commission (IWC), 2001). DNA sequencing revealed that the differences between these two species are greater than those between other acknowledged species in the same genus, and therefore warrant the recognition of the Antarctic minke as a distinct species (Arnason et al., 1993).

The Antarctic minke whale is in the large baleen whale family, *Balaenopteridae*, often known as 'rorquals' from the Norse word meaning 'whale with pleats in its throat' referring to the large ventral grooves on the lower jaw (Bannister, 2002). Antarctic minke whales have relatively short heads, less than a quarter the length of the body, short and wide baleen plates, a narrow and pointed rostrum (snout), and short pectoral fins (Bannister, 2002). Mature female Antarctic minke whales are estimated to average 9 m in length, while the males average 8.5 m (Perrin & Brownell, 2002).

In the Antarctic, minke whales feed primarily on euphausiids, such as Antarctic krill (*Euphausia superba*) (Laws, 1977). Rorqual feeding behavior consists of lunge filter feeding, a process in which a large volume of water and prey are engulfed and then filtered through the baleen plates (Goldbogen et al., 2012). While lunge feeding, these whales approach their prey at high speed, open their mouths wide, thereby allowing the ventral grooves in their throat to inflate the buccal cavity and maximize prey consumption (Brodie, 2001). It has been shown that engulfment duration and metabolic expenditure is proportional to body size (Potvin et al., 2010). Therefore, Antarctic minke whale foraging is characterized by shallower dives, higher lunge frequencies, and lower metabolic cost compared to larger baleen whales. Particularly high feeding rates have been observed in minke whales that are hunting krill under sea ice (Friedlaender et al., 2014). Antarctic minkes are known to take advantage of sea ice habitat where their small size and short fins allow for greater maneuverability to exploit krill in the pack ice (Friedlaender et al., 2014) and to avoid predation. *Orcinus orca*, commonly known as killer whales, have been known to prey on minke whales, particularly young calves and juveniles, in the Southern Ocean (Perrin & Brownell, 2002; Pitman & Durban, 2012). Due to their position in the middle trophic level of the Antarctic ecosystem, being both predator and prey, and their relatively small size compared to other baleen whales, the Antarctic minke whale is considered a mesopredator.

Antarctic minke whales have a circumpolar pelagic, or open water, distribution in the Southern Hemisphere. It has long been known that minke whales specifically prefer sea ice habitats (Laws, 1977), but evaluating population sizes has remained difficult in the dynamic pack ice. Historically, cetacean, or marine mammal, population surveys have been conducted by vessels unable to penetrate sea ice, so minke whales were often found in an association with the sea ice edge. With the use of icebreakers, however, it is clear that this species also occurs throughout the ice pack and within polynyas (areas of open water surrounded by sea ice) (Ainley et al., 2007, 2012). Icebreaker-supported helicopters are allowing scientists to extend the reach of population surveys into the marginal ice zone to provide a more holistic description of minke whale habitat preference. Williams et al. (2014) found that most minke whales are present within the ice edge zone during the summer months, and they predict that approximately 20% of the population in the Weddell Sea region are located in the difficult to navigate and survey marginal ice zone and farther into the pack ice. This distribution is consistent with the dense patches of Antarctic krill located 13 km south of the ice edge (Brierley et al., 2002), which likely influences minke whale distribution (Friedlaender et al., 2006).

Daily movements of Antarctic minke whales have not been studied, yet their seasonal distributions have been observed. During the austral summer and fall months, between December and May, Antarctic minke whales can be found feeding within the pack ice south of 60°S. Their winter distribution is less known, but some of the population does remain in Antarctic waters during the winter months (Ensor, 1989). Records from whaling vessels indicate that a proportion of the population, however, is believed to migrate to winter breeding grounds in more northern latitudes (Perrin & Brownell, 2002). One such wintering area is located off the coast of northern Brazil (7°S), where a 1964-1985 whaling operation mostly targeted minke whales, with a peak in October (Da Rocha & Braga, 1982). Data from Japanese scouting vessels have described a high abundance of minke whales in the central South Pacific (10°-30°S) in November and in the eastern and southern Indian Ocean between the equator and 50°S (Miyashita et al., 1995). Whaling records prior to the 1990s classified all minke whales as one species (*B. acustorostrata*), so the proportion of these catches that were actually *B. bonaerensis* (Antarctic minke whales) is unclear. Modern observations are scarce and annual migration patterns are mostly unknown for the Antarctic minke whale.

Social behavior and life history of the Antarctic minke whale are also not well studied, yet they have been observed in solitude or small groups of two or three individuals. Females reach sexual maturity at 7 to 8 years and males at 8 years of age. The pregnancy rate of adult females approaches 90%, suggesting an average annual cycle with peak births in July and August (Horwood, 1990). During the summer and fall feeding season, mature females are found closer to the ice than immature females and immature males are more solitary than mature males (Perrin & Brownell, 2002).

Antarctic minke whales were largely ignored during industrial whaling due to their small size, but after 1979, as the stock of larger rorquals was depleted, the IWC only permitted factory ships to take minke whales as their population was deemed stable. The minke whales' pagophilic, or ice-loving, nature may have also protected them during industrial whaling, which allowed their population to remain stable compared to other targeted species such as humpback and fin whales (Ainley et al., 2007; Tonnessen & Johnsen, 1982). During this period of targeted whaling, annual catches of minke whales in the Southern Ocean reached 8000 by Japan and the USSR (Horwood, 1990). The 1985/1986 Antarctic season marked the end of commercial whaling under the IWC moratorium. Between 1992 and 2004, the IWC Scientific Committee estimated the Antarctic minke whale population was reduced to 515,000 from the 1985-1991 estimation of 720,000 individuals (International Whaling Commission (IWC), 2002). A large investigation, beginning in 2013, is currently underway to obtain an accurate estimation of the minke whale population in the Southern Ocean as the Japanese continue their lethal sampling of this species (Normille, 2015).

1.1.2 Japanese Whale Research Program

As the most abundant cetacean in the Southern Ocean, Antarctic minke whales have been the target of a long-term, contentious lethal sampling program undertaken by the Japanese Whale Research Program under Special Permit in the Antarctic (JARPA). The IWC used to set catch limits for commercial whaling under the 1946 International Convention for the Regulation of Whaling. In 1982, however, the IWC established a commercial whaling moratorium that is still in place today (Gales et al., 2005). Nevertheless, JARPA continue to defend their methods, arguing that the collection of genetic samples is necessary for determining population structure and can only be obtained through lethal sampling, which is permitted through the International Convention for the Regulation of Whaling for scientific research purposes (Gales et al., 2005). Non-lethal biopsy techniques, however, have been used in DNA analysis for age estimation in humpback whales (Polanowski et al., 2014), and could be used in the Southern Ocean to more efficiently and humanely study minke whale population structure. One of the largest criticisms against Japan's scientific whaling program is that it occurs within the IWC's Southern Ocean Whale Sanctuary (Figure 1.1), where whaling is strictly prohibited in order for scientists to study whale populations unaffected by and recovering from commercial whaling (Gales et al., 2005).

In March of 2014, the United Nations International Court of Justice ruled that scientific research did not justify lethal sampling and ordered Japan to halt all whaling in the Southern Ocean (Normille, 2015). Japan's new proposal, initiated in the 2015/2016 season, reduces the annual cull of minke whales from 900 individuals to 333 for the next 12 years (Normille, 2015). An expert panel for the IWC reviewed the new proposal in February 2015 and claimed that their two main research objectives (calculating population sizes in order to return to sustainable commercial hunting, and gaining a better understanding of the Southern Ocean ecosystem) did not demonstrate a need for lethal sampling (Normille, 2015). Despite this ruling, JARPA resumed their hunt in December 2015 after a year-long hiatus. The whaling fleet returned to Japan in March of 2016 with 333 Antarctic minke whales, 207 of which were pregnant females (Izadi, 2016). The IWC is expected to meet in autumn of 2016 for a proposed revision.

1.2 Development of Animal Movement Analysis

Wildlife tracking helps scientists and conservationists remotely observe individual and population movement patterns within local areas as well as migration patterns across continents and oceans. Technologies used to track wildlife have developed considerably from the first systematic studies of animal movement in the early 20th century, when scientists began to attach identification bands to migratory birds returning to the same location each year (Nebel, 2010). In the late 1950s, radio transmitters were used to track wildlife, and in 1978, the Advanced Research and

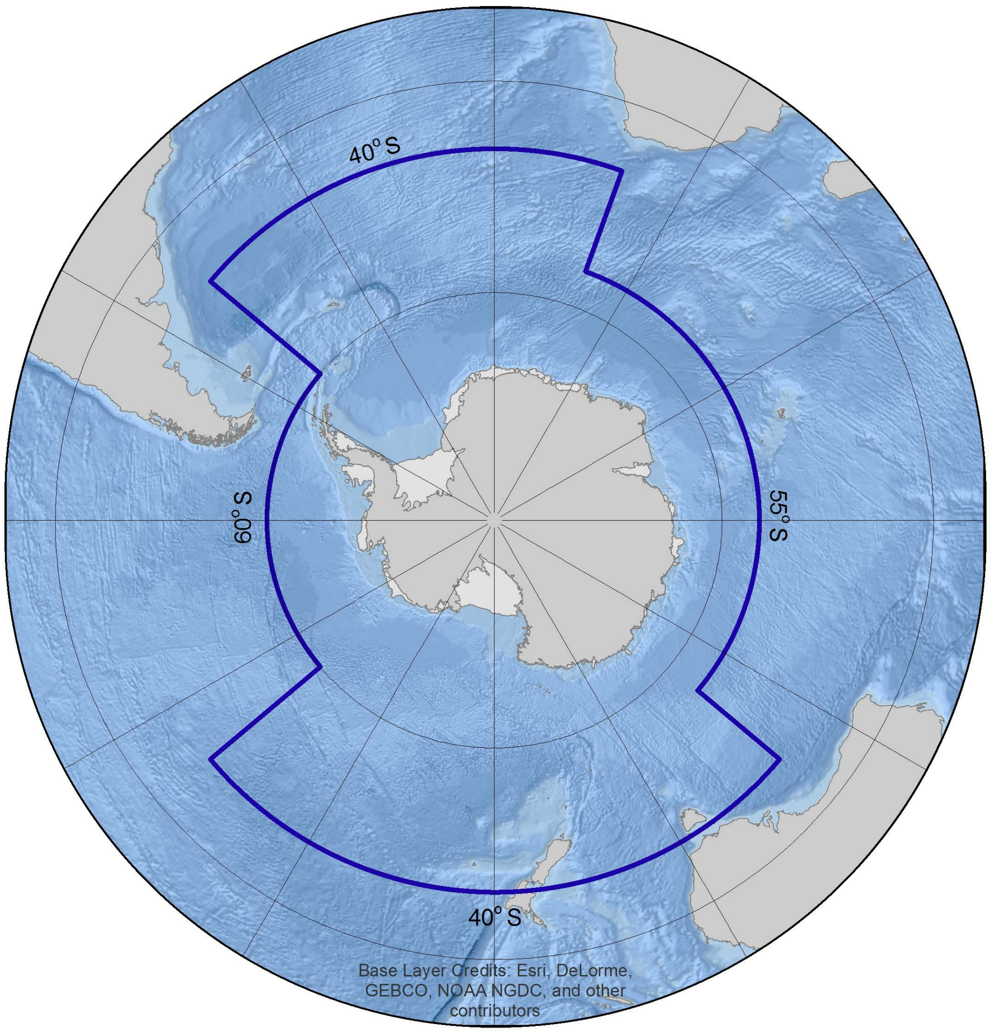

Figure 1.1: Southern Ocean Whale Sanctuary boundary as defined by the IWC. Whaling for any purpose is strictly prohibited south of this boundary.

Global Observation Satellite (ARGOS) system provided a method for automatically tracking animals globally. The early 1990s then brought the Global Positioning System (GPS), which allows for high-resolution tracking data (Nebel, 2010).

Today, satellite tracking offers the most detailed method for studying long distance migration and daily behavioral changes over extended periods of time and in difficult to survey locations. The availability of this behavioral and spatial data is scarce for most marine organisms, especially baleen whales, but is necessary for gaining a holistic understanding of these large, migratory species. Daily movement patterns of Antarctic minke whales are not well documented and largely unknown due to their cryptic behavior, the remoteness of Antarctica, and the difficult to maneuver and survey pack ice habitat that these whales prefer. The present study provides the first use of satellite telemetry in studying Antarctic minke whale movements and behavior in the Southern Ocean.

1.3 Ice-Ocean-Atmosphere Interactions

Satellite observations and climate models, developed in the 1970s, have allowed us to study interannual sea ice variability and the relationships between ice and climate around the Antarctic continent with greater accuracy and resolution than shipboard measurements of the past (Cavalieri, 2003; Zhang, 2007; Zwally et al., 2002). Annual fluctuations in sea ice extent, concentration, and thickness are key factors influencing Antarctic marine ecosystems, particularly in determining the location and timing of phytoplankton blooms (Smith et al., 2008). Changes to this vulnerable system may be detrimental to marine life and can influence the global climate. Sea ice plays an important role in the global climate by reducing heat and moisture exchange between the ocean and atmosphere, increasing regional albedo, and regulating temperature and salinity in the polar oceans, thereby maintaining the global meridional overturning circulation (MOC). The cold, dense, bottom water of the MOC is formed in the North Atlantic Ocean as well as the marginal Ross and Weddell Seas around Antarctica (Fahrbach et al., 1995). Particularly in the Southern

Ocean, near the Antarctic continent, strong katabatic winds blow off the ice sheet and continent, advecting sea ice northwards, and creating polynyas. These polynyas experience high winds and cool air temperatures, which forms new ice and results in brine rejection into the underlying waters. The high salinity content of these waters is the primary driver of dense water formation on the shallow continental shelf (typically 500 m) to form Antarctic Bottom Water, a key driver in the MOC (Heywood et al., 2014). Due to the greater distance from the geographic pole, Southern Ocean sea ice is affected by stronger solar radiation than Arctic sea ice and therefore experiences different melting rates and processes, such as freeboard flooding as opposed to Arctic melt ponds (Bernstein et al., 2015).

Antarctic sea ice cover experiences significant annual advances and retreats from a maximum of approximately 19 million km^2 in September to a minimum of approximately 3 million km^2 in February (Cavalieri & Parkinson, 2008). These seasonal fluctuations are dominated by the atmospheric semi-annual oscillation (SAO), which is characterized by a biannual expansion and contraction of the circumpolar pressure trough in spring and autumn (Stammerjohn, 2003). The strength of the SAO varies on interannual to decadal time scales, and its three-wave variability introduces longitudinal differences in atmosphere-ocean-ice exchange around the continent (van den Broeke, 2000). This variability can explain different temperature trends between East Antarctica and the Antarctic Peninsula. The amplitude of the SAO and winter sea ice extent west of the Antarctic Peninsula is strongly coupled. During a weakened SAO, the northwestward propagation of the circumpolar pressure trough is suppressed, increasing mean wind speeds and cloudiness, which causes negative sea ice anomalies and regional warming in the Amundsen and Bellinghausen Seas (van den Broeke, 2000).

The western Antarctic Peninsula demonstrates a strong climatic response to atmospheric and upper ocean circulation anomalies because of its direct exposure to the South Pacific. Fluctuations in sea ice advance in the western Antarctic Peninsula region have also been associated with decadal changes in the Southern Annular Mode

(SAM) and high latitude responses to the El Niño Southern Oscillation (ENSO). ENSO, a global-scale climate pattern, in the tropical Pacific develops a strong circulation teleconnection with the Southern Ocean, particularly in the Pacific sector, on an intraseasonal and interannual timescale (Stammerjohn et al., 2008b). The SAM, also known as the Antarctic Oscillation (AAO), is characterized by the changing location of the westerly wind belt, affecting the strength and position of cold fronts and mid-latitude storm systems. Positive SAM phases are demonstrated by positive atmospheric pressure anomalies at mid-latitudes, negative atmospheric pressure anomalies at high latitudes, and are concurrent with El Niño phases, and the opposite is true for negative SAM phases that co-occur with La Niña phases (Stammerjohn et al., 2008b).

1.4 Recent Warming Trends

Between the 1950s and 1980s, the Southern Ocean has experienced a rapid warming of at least 0.17°C , which is greater than that of the global ocean (Gille, 2002). This warming is mainly concentrated in the Antarctic Circumpolar Current and is comparable to Southern Ocean atmospheric temperature increases (Gille, 2002). The Antarctic Peninsula is oriented north to south and positioned in the Antarctic Circumpolar Current, resulting in direct exposure to the prevailing westerlies, and making it particularly responsive to rapid climate change. This region, as the most rapidly warming climate in the Southern Hemisphere (Gille, 2002), shows an increase in atmospheric temperature of 0.56°C/decade over the past 50 years (Turner et al., 2005).

Passive microwave satellite measurements show a slight increase in average annual sea ice extent around Antarctica since 1979 (Cavalieri & Parkinson, 2008). The Southern Ocean and atmosphere, however, show a warming trend around a significant portion of the continent (Zhang, 2007). Despite an overall increase in sea ice cover around Antarctica, the Amundsen-Bellinghausen Seas, on the western side of the Antarctic Peninsula, have experienced a reduction in sea ice extent and growing season between 1979 and 2004. Sea ice in this region is retreating 31 ± 10 days earlier and advancing 54 ± 9 days later, resulting in a shorter sea ice season (Stammerjohn et al., 2008b). Stammerjohn et al. (2008a) show that key ice-ocean-atmosphere interactions and trends in the western Antarctic Peninsula and Bellinghausen Sea are consistent with the rapid warming of the Antarctic Peninsula region. The tendency for a later autumn ice advance is associated with increased winds blowing from low latitudes that advect warm air from the subtropics into the region, restricting ice growth against the Antarctic coast and increasing ocean heat flux with the atmosphere. The shorter sea ice season is also coincident with the decreased trend in monthly sea ice concentration and increased interseasonal sea ice variability, suggesting thinner sea ice and increased ocean heat flux to the atmosphere during the winter (Stammerjohn et al., 2008a). Since most polar marine organisms' life histories are coupled with the seasonal cycle of sea ice, these changes are expected to affect the ecosystem functionality of the western Antarctic Peninsula region.

1.5 Purpose of This Study

As a pagophilic mesopredator, the Antarctic minke whale plays a vital role in the ecosystem of the Antarctic pack ice. Understanding the ecology and migration patterns of cetacean species in the Southern Ocean is vital for interpreting the impacts of global climate change on polar marine ecosystems. With their slim, compact body, small fins and hard, pointed rostrum, the Antarctic minke whale is suited for life in the pack ice. Smaller and more specialized for exploiting sea ice habitats than the humpback and fin whales that share the Southern Ocean during the summer feeding season, the Antarctic minke whale has been observed within the MIZ, most likely hunting krill under the sea ice. The coupled relationship between minke whales, krill, and sea ice suggests that these whales will be sensitive to changes in sea ice concentration, extent, and duration, making them particularly vulnerable to climate change. Evaluating this species' habitat preferences and population dynamics is also necessary for developing appropriate conservation and management practices, especially as this species is the subject of a contentious ‘scientific’ lethal sampling program undertaken by the Japanese Whale Research Program.

Little is known about the daily movements of Antarctic minke whales. It is known that they prefer sea ice habitat, but due to the restrictions of ship observations and limited availability of icebreaker-supported helicopters, this hypothesis has not been rigorously tested. The aim of this study is to investigate this information using satellite tags attached to Antarctic minke whales. The positions of the whales during the foraging season will also be combined with remote sensing data to estimate the relationship between whale behavior and the environment. We hypothesize that Antarctic minke whales will distribute themselves exclusively within the marginal ice zone throughout the feeding season and then migrate to more northerly waters.

Chapter 2
DATA PREPARATION

2.1 Satellite Tracking Data

The ARGOS satellite system was established in 1978 as a collaboration between the French Space Agency (CNES), the National Oceanic and Atmospheric Association (NOAA), and the National Aeronautics and Space Administration (NASA), and is currently operated and managed worldwide by CLS (Collecte Localisation Satellites), a subsidiary group of CNES. The ARGOS system uses six polar orbiting satellites to collect data from satellite tags known as Platform Terminal Transmitters, PTTs, and provides sensor and location data to the user. The accuracy of the location data is dependent on the number of ARGOS satellites that are in view while the tag is on the surface. Location quality classes 1, 2, and 3 are accurate to within 500-1500 m, 250 m, and 100 m, respectively. Classes 0, A, and B are locations with no associated error estimation.

Antarctic minke whales were tagged with battery powered SPOT-5 implantable tags, produced by Wildlife Computers (Redmond, WA), in Wilhelmina Bay, on the western coast of the Antarctic Peninsula, on 9 February 2013 by Dr. Ari Friedlaender and colleagues. Similar to Gales et al. (2009), the tags were attached to the back of the whale, adjacent to the dorsal fin, which allowed the tag to break the surface of the water, trigger the salt water switch, and communicate with the satellite when the whale surfaced to breathe. The tags were duty cycled to attempt to resolve a location every time the whale was at the surface during a four hour period, and then turned off for eight hours. Each location was filtered based on its location quality class for spatial and temporal accuracy and run through a first difference correlated random walk model (DCRW), to define a specific time step, in R: A Language and Environment for Statistical Computing (Jonsen et al., 2014; R Development Core Team, 2016), which generated four points per day, every six hours, for each whale. *In situ* abiotic data were not recorded with the ARGOS satellite tags. Therefore, remote sensing datasets were used to detect potential covariates between whale movements and environmental conditions.

2.2 Sea Ice Data

2.2.1 Sea Ice Concentration

Sea ice concentration is the fraction of ocean area covered by sea ice, ranging between 0 and 100%. The National Snow and Ice Data Center (NSIDC)[1] archives daily sea ice concentration data. A consistent time series of sea ice concentration is generated from brightness temperature data derived from the Defense Meteorological Satellite Program (DMSP)-F17 Special Sensor Microwave Imager/Sounder (SSMIS) using the NASA Team Sea Ice Algorithm. Accuracy estimates of the algorithm vary depending on sea ice conditions and locations. Generally, the accuracy of total sea ice concentration is within ± 5% of the actual sea ice concentration, and is more accurate when ice concentration is high and sea ice thickness is greater than 20 cm (Cavalieri et al., 1992).

Data are stored in 8-bit binary files as one-byte integers representing sea ice concentration values. Derived fractional sea ice concentration floating-point values, ranging between 0.0 and 0.1, are multiplied by a scaling factor of 250 in byte format. For example, a concentration value of 0.0 (0%) is stored with a one-byte integer value of 0, and a concentration value of 1.0 (100%) is stored with a one-byte integer value of 250. In order to obtain the fractional parameter, the one-byte integer values can be divided by 250. Data files may contain integers ranging from 0 to 255, as described in Table 2.1.

[1] http://nsidc.org/data/NSIDC-0051/versions/1

Table 2.1: Description of NSIDC sea ice concentration data values.

Data Value	Description
0 - 250	Sea ice concentration (fractional coverage scaled by 250)
251	Circular mask used in the Arctic to cover the data gap around the pole (caused by the satellite's orbit inclination and instrument swath)
252	Unused
253	Coastlines
254	Superimposed land mask
255	Missing data

For the present study, gridded daily average sea ice concentrations for the south polar region were obtained with a grid cell size of 25 x 25 km. The data were stored as one-byte integers in flat binary arrays. In order to analyze the data in a geographic information system (GIS) such as the Environmental Systems Research Institute's (ESRI) Desktop ArcGIS (ESRI, 2015), the data required preprocessing. First, the file extension was changed from .bin to .bil. A header file was created to define the properties of the raster such as number of rows and columns, number of bands and bits, and the x and y coordinates of the origin. The .bil files were then converted to a compatible grid raster format, such as TIFF, using the ArcMap tool *Raster to Other Format (multiple)*. Finally, the South Pole Lambert Azimuthal Equal Area projection was defined. This process was completed for each daily sea ice concentration grid for the study period between 9 February and 8 June 2013, a total of 120 days, using a Python script. Finally, sea ice concentration grids, as well as additional environmental data, were restricted to the study area south of 60°S and between 30°W and 150°W(Figure 2.1).

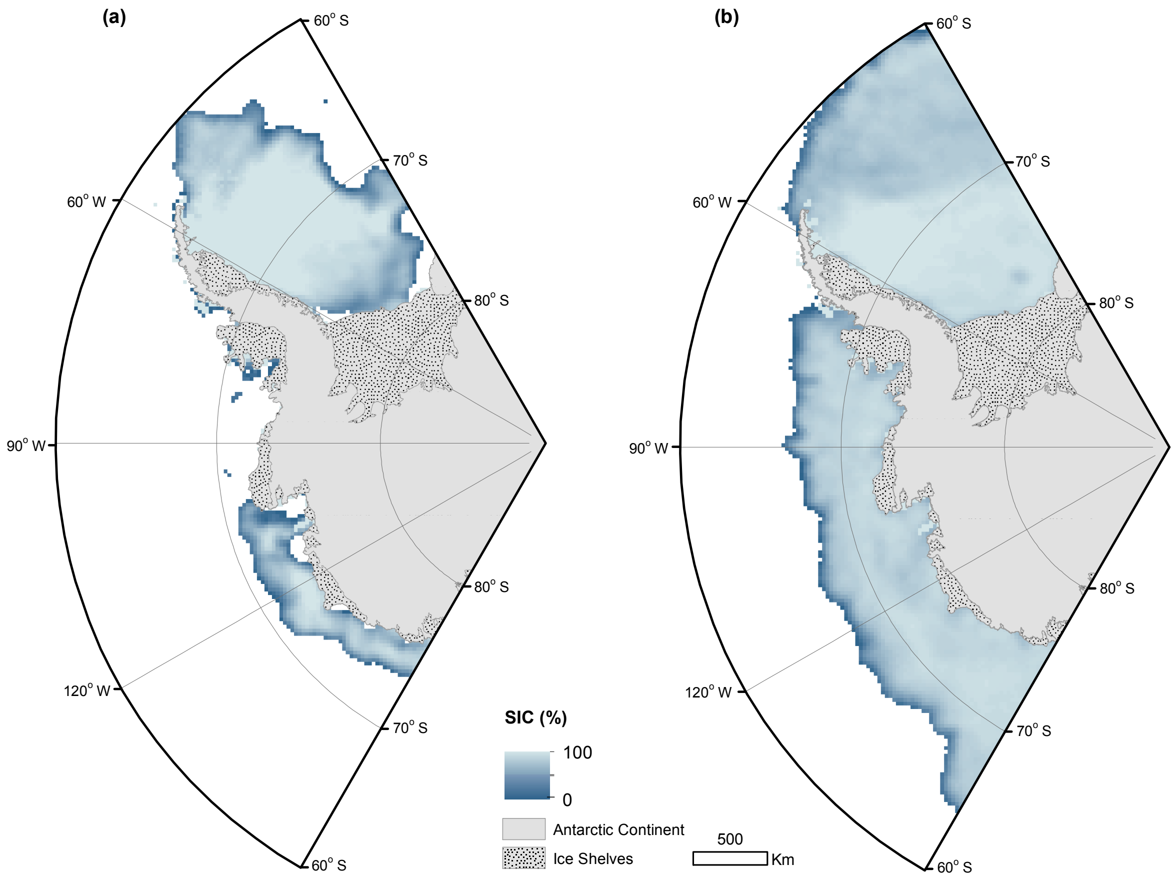

Figure 2.1: Sea ice concentration around the western Antarctic Peninsula on (a) 9 February and (b) 8 June 2013.

2.2.2 Sea Ice Extent

Sea ice extent is defined as the total area of ocean covered by at least 15% sea ice concentration. The National Ice Center (NIC)[2] provides daily shapefiles of sea ice extent and the marginal ice zone, which is the transition between the sea ice extent and open ocean. The marginal ice zone is very dynamic, depending on local wind directions and ocean currents, and it plays an important role in ice-ocean-atmosphere interactions. Expert sea ice analysts use multiple satellite imagery sources including passive and active microwave, visible, and infrared sensors to create composite ice charts as GIS-compatible shapefiles with a spatial resolution down to 50 m (Dedrick et al., 2001). For this study, daily sea ice extent shapefiles for the period between 9 February and 8 June 2013 (Figure 2.2) were downloaded from NIC as polygon (vector) layers and brought into ArcGIS for analysis.

2.2.3 Sea Ice Thickness

Sea ice thickness was calculated from biweekly sea ice concentration charts provided by the National Ice Center (NIC) using the procedure developed by DeLiberty et al. (2011). Ice charts identify the ice concentration and ice type for each polygon following the World Meteorological Organization (WMO) classification system (World Meteorological Organisation (WMO), 1970). WMO ice types, described in Table 2.2, are defined by their physical characteristics over a range of thicknesses, corresponding to their stage of development, also referred to as ice type. Using the WMO nomenclature and range of thicknesses, we calculated the mean thickness, $\bar{z}$, in a given polygon using the equation:

$$\bar{z} = \sum_{i=1}^{b} c_i z_i \tag{2.1}$$

where z_i is the mean thickness and c_i is the weighted concentration within each thickness bin, b. All ice types were binned into thickness ranges of 0 - 0.1, 0.1 - 0.3,

[2] http://www.natice.noaa.gov/Main_Products.htm

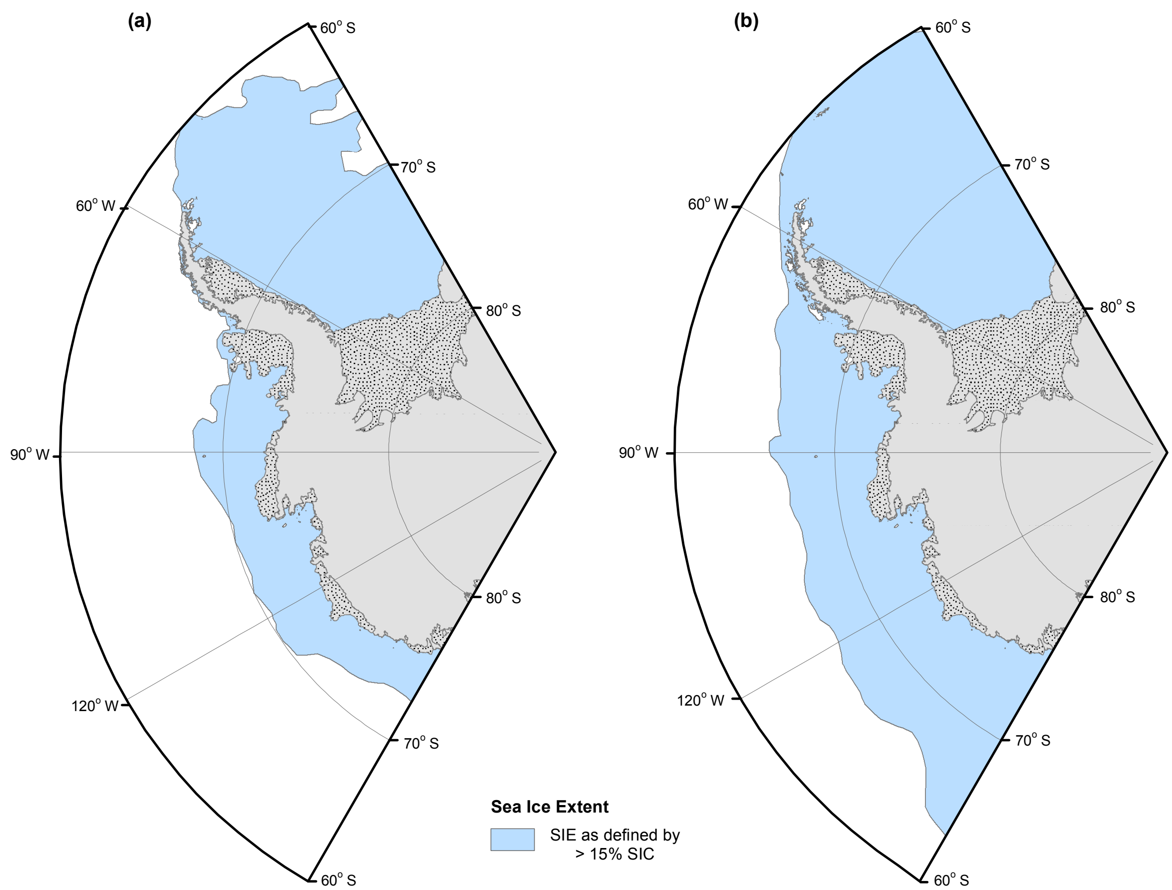

Figure 2.2: Sea ice extent around the western Antarctic Peninsula on (a) 9 February and (b) 8 June 2013.

Table 2.2: World Meteorological Organization sea ice thickness classifications, adapted from DeLiberty et al. (2011).

Thickness Range (m)	Stage of Development	Description
0	Ice Free	Open water
0 - 0.10	New Ice	Ice crystals weakly frozen together
	Nilas	A thin elastic covering of ice that can bend with waves and has a matte surface
	Pancake Ice	Circles of ice 0.3 - 3 m in diameter with thicker brims
0.10 - 0.30	Young Ice	Ice in transition between nilas and first-year ice
0.30 - 0.70	Thin First-Year	Thin first-year ice that has grown over not more than one winter
0.70 - 1.20	Medium First-Year	Medium thick first-year ice
>1.20	Thick First-Year	Thickest first-year ice
	Old Ice	Ice surviving at least one summer melt

0.3 - 0.7, 0.7 - 1.2, and >1.2 m, as seen in Figure 2.3. Due to its coarse temporal resolution, sea ice thickness was not correlated with whale movement but was instead used to understand sea ice dynamics in the study region.

2.3 Additional Environmental Data

2.3.1 Sea Surface Temperature

Daily optimally interpolated sea surface temperature (OISST)[3] is a regular global sea surface temperature product constructed by blending observations from different sources, such as satellites, ships, and buoys. Interpolation is used to fill gaps in order to produce a spatially complete $\frac{1}{4}$ x $\frac{1}{4}$ degree daily grid. Satellite imagery is

[3] https://www.ncdc.noaa.gov/oisst

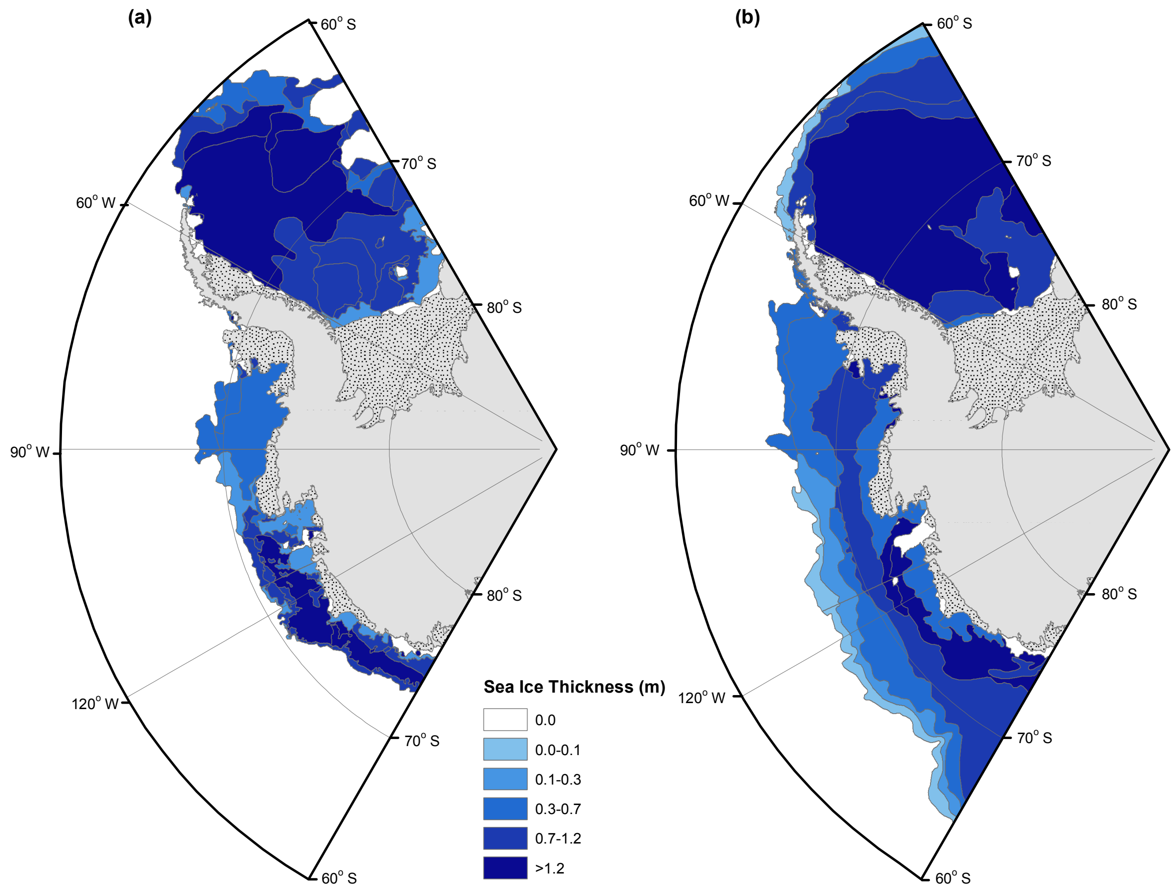

Figure 2.3: Sea ice thickness around the western Antarctic Peninsula during (a) the first week of February and (b) the first week of June, 2013.

provided by the Advanced Very High Resolution Radiometer (AVHRR) infrared instruments. Comparisons with sea ice concentration grids are used to simulate and interpolate SSTs adjacent to and under sea ice cover. Undetected sea ice, however, is known to cause unrealistically warm OISSTs, particularly near the ice edge where the ice is patchy and not fully solidified. These areas are ideal foraging locations for Antarctic minke whales, which may cause discrepancies between our model predictions and our current knowledge of minke whale habitat.

Archived daily Network Common Data Form (netCDF) files were gathered for this study during the period between 9 February and 8 June 2013 (Figure 2.4). The netCDF layer containing the entire study period was brought into ArcMap and then individual netCDF raster bands were exported as TIFFs for each day using a Python script.

2.3.2 Bathymetry

Bathymetry is the depth of the ocean and is equivalent to underwater topography. The International Bathymetric Chart of the Southern Ocean (IBCSO)[4] program is a regional mapping project of the General Bathymetric Chart of the Oceans (GEBCO). The digital bathymetric model provides a better understanding of the sea floor topography of all circum-Antarctic waters by collecting and compiling bathymetric data from over 30 institutions and 15 countries. Bathymetry was measured with multibeam and single-beam echo soundings, digitized nautical charts, regional bathymetric gridded compilations, and predicted bathymetry. The resultant model is publicly available as a GeoTIFF with a spatial resolution of 500 x 500 m in the World Geodetic System 1984 Antarctic Polar Stereographic projection covering the region south of 60°S (Figure 2.5).

[4] http://www.ibcso.org/data.html

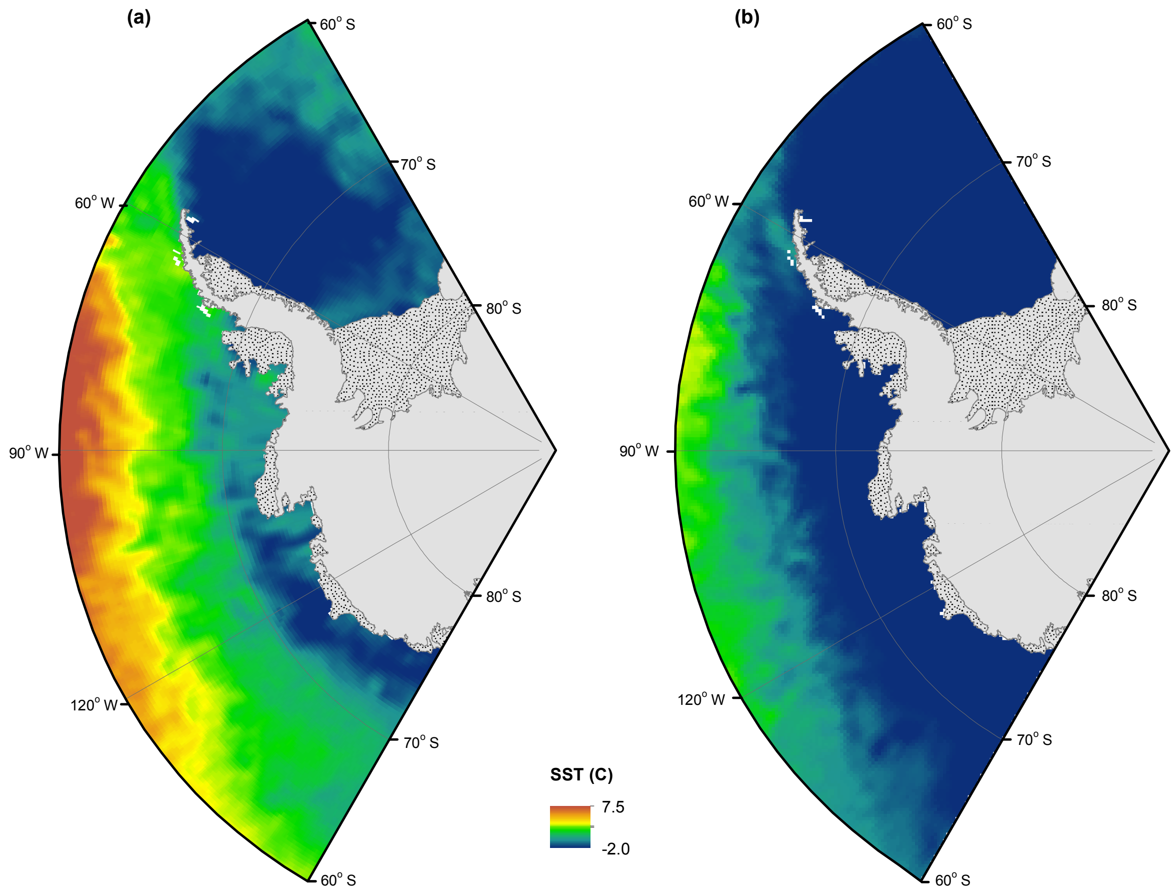

Figure 2.4: Sea surface temperature around the western Antarctic Peninsula on (a) 9 February and (b) 8 June 2013.

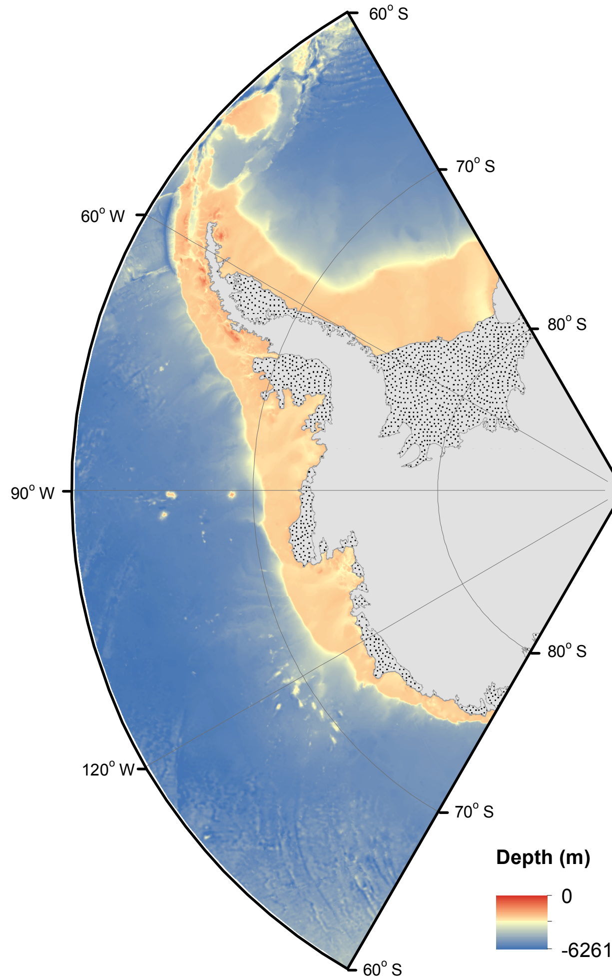

Figure 2.5: Bathymetry around the western Antarctic Peninsula.

Chapter 3

METHODOLOGY

3.1 Satellite Tag Deployment

ARGOS satellite transmitters were attached to three Antarctic minke whales in Wilhelmina Bay, on the western coast of the Antarctic Peninsula on 9 February 2013, at approximately 62°14'50"S 64°41'09"W, 62°14'30"S 64°41'22"W, and 62°15'09"S 64°38'11"W (Table 3.1). Individuals with ID numbers 112745, 112747, and 112750 will be referred to as Whales 1, 2, and 3, respectively, throughout the text of this document.

Every day throughout the study period, the satellite tags were active for four hours and inactive for eight hours. Each time a satellite passed over the whale during the active four hours, and the whale surfaced during this time, an attempted location was transmitted. This process resulted in a patchy distribution of points with inconsistent time steps between locations. In order to regularize the data to four points per day, every six hours (Figure 3.1), Dr. Friedlaender and colleagues used a Bayesian state-space model to generate a first-difference correlated random walk (DCRW) in R (Jonsen et al., 2014; R Development Core Team, 2016). In animal movement data, the direction is persistent and therefore does not represent a true random walk, or autoregressive model. Instead, a correlated random walk is performed in which the direction chosen at step i+1 is related to the direction at step i. The random aspect of this model is the change in direction from step i to step i+1, which is referred to as the turning angle.

Table 3.1: Details of ARGOS satellite tags deployed on three Antarctic minke whales on 9 February 2013.

Deploy ID	Last Transmission	Days Active	Total Points (ARGOS)	Modeled Points (DCRW)	Track Length (km)
112745	29 May 13	109	2,662	436	6,401
112747	31 May 13	111	1,738	443	12,543
112750	8 August 13	180	3,001	719	13,152

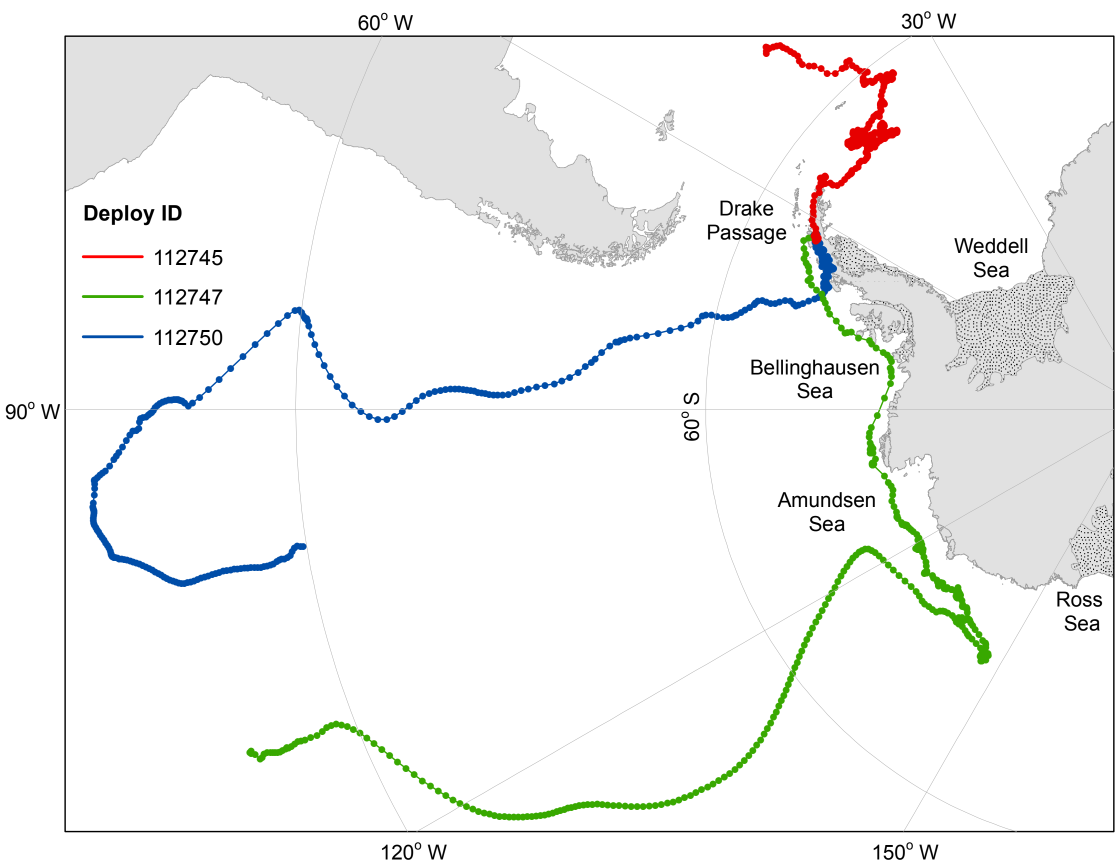

Figure 3.1: Trajectories of three Antarctic minke whales tagged in 2013. Tracks show results of the first difference correlated random walk model with a step interval of 6 hours.

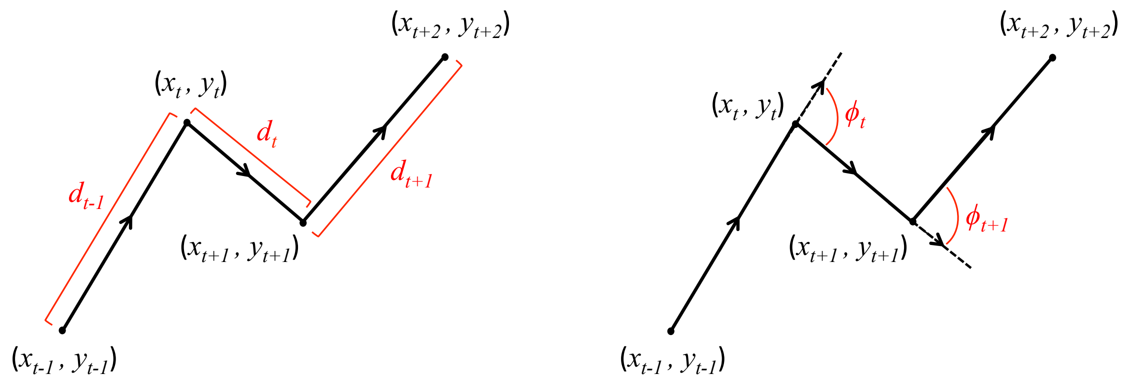

Figure 3.2: Illustration of step distance (d) and step turning angle (ϕ) between time steps (t).

3.2 Analyzing Movement Data

In order to analyze and visualize the whales' tracks, we used a series of functions provided by the *move* package in R (Kranstauber & Smolla, 2016). The minimum requirements for utilizing the move package are time-stamps, coordinates, and a unique ID for each animal, however additional information can be stored within the move object such as demographic data or, for this study, environmental data.

The move package includes functions to calculate distance, speed, angle, and turning angle between time steps, which for this study, is an interval of 6 hours (Figure 3.2). The angle is defined as the direction of movement, while the turning angle is the change in angle. As well as computing step behaviors for each whale, the move package also calculates their utilization distributions with the dynamic brownian bridge movement model. This model develops an estimation of an individual's home range by incorporating temporal and behavioral characteristics of the whales' movement patterns. Utilization distributions were calculated when the whales were considered in a foraging state, as defined by the Multi-Scale Straightness Index.

3.2.1 Multi-Scale Straightness Index

Track tortuosity, or the degree to which a track deviates from a straight line, can help characterize different behavioral states, such as resting, migrating, or foraging. With the advancement of tracking technologies such as GPS and ARGOS satellite telemetry, we are now able to remotely acquire large quantities of movement data at fine spatiotemporal scales. From these observational data consisting of time-stamped location information, we can compute step lengths, speeds, and turning angles. However, we are often also interested in behavioral states and how they change over time. Tortuosity can be extracted from animal movement data using the straightness index, sinuosity, and fractal dimension.

In this analysis, tortuosity is evaluated using the Multi-Scale Straightness Index (MSSI) developed by Postlethwaite et al. (2013). The MSSI is an adapted version of the Straightness Index, which is defined as the ratio of the beeline distance between the first and last track location to the total length of the traveled trajectory. Instead of evaluating the degree of straightness over the entire track, the MSSI computes track straightness multiple times and over a range of time scales, permitting the identification of distinct behavioral states throughout the track.

To compute the MSSI, each track was analyzed at intervals equal to the fixed 6-hour time step (s) between points previously derived from the DCRW model. These intervals are referred to as the granularity (g), or the temporal resolution at which we viewed the track. The observational sliding window (w) is the length of time over which we computed the MSSI. The window must be a multiple of the granularity, and both are multiples of the time step. The MSSI is then defined by the equation below:

$$S(t_j + \frac{w}{2}, g, w) = \frac{d_j(w)}{\sum_{k=0}^{s_2-1} d_{j+ks_1}(g)} \tag{3.1}$$

The first argument of S is the time at which the MSSI is defined and is shifted to be in the center of the window, the second argument is the granularity, and the third argument is the window. The numerator is the great circle distance between two

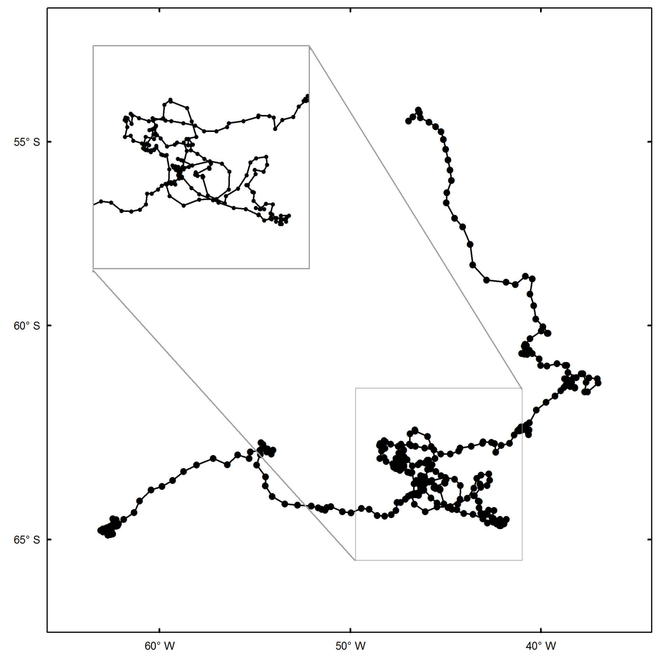

Figure 3.3: Trajectory of 112745 demonstrating the use of MSSI for detecting behavioral changes. Inset shows an enlargement of area-restricted behavior.

locations at the time interval of w, and the denominator is the total distance traveled between the same two locations when viewed at the time interval of g. The value of S is always between 0 and 1, where values close to 0 indicate more tortuous tracks and values close to 1 indicate less tortuosity. Figure 3.3 demonstrates Whale 1's trajectory with sections of approximately straight-line movement that correspond to large values of S and sections of area-restricted movement that would correspond to lower values of S.

Careful consideration must be taken when defining the size of the window. Postlethwaite et al. (2013) recommend choosing the parameters after examining the MSSI over the entire track length. Values should be chosen to represent the temporal scale of the desired behavioral states in order to identify changes in behavior. One major limitation of this dataset is the timestep between location points. Six hours may be too coarse of a temporal resolution to identify each feeding bout during the day. A larger window, however, can compensate for this limitation by encompassing

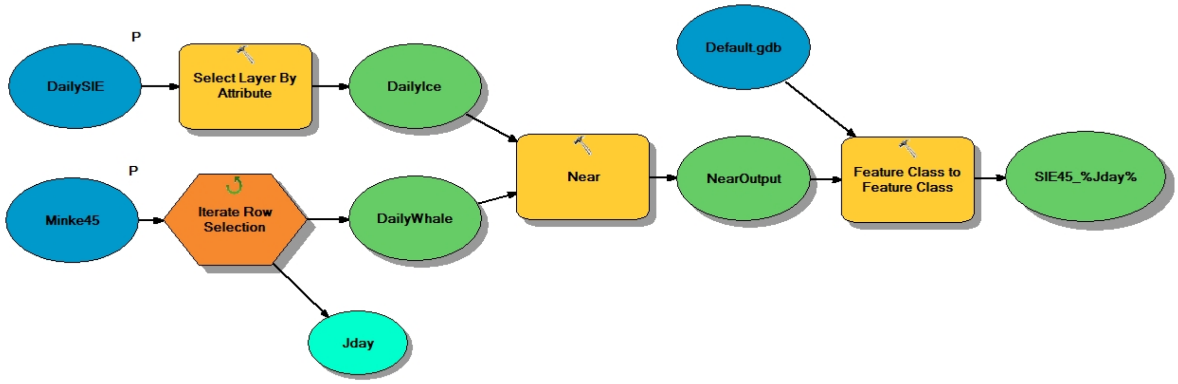

Figure 3.4: Schematic of ArcGIS ModelBuilder used to determine distance to the sea ice extent.

multiple bouts of the same behavior and providing an indication of the predominant behavior during that time. Therefore, we used a granularity of 1 timestep (every 6 hours) and a window size of 25 points, which equates to approximately 6 days. The results of our analysis will therefore provide behavioral state information on a multi-day to weekly scale rather than a fine scale, hourly analysis.

3.3 Distance to Sea Ice Extent

Daily distance to the sea ice extent was calculated using ArcGIS ModelBuilder (Figure 3.4). The *Near* tool calculated the euclidean, or straight-line, distance between features. The row iteration too was used to loop through the timestamps in the whale location data in order to be matched with the correct ice extent through its corresponding Julian day. Results were saved as a new shapefile containing four distance calculations per day for each whale. During the initial few weeks of each trajectory, the whales were within the bays along the Western Antarctic Peninsula, where the ice was gradually advancing. The Weddell Sea on the Eastern side, however, contained vast amounts of sea ice. The *Near* tool in ArcGIS was unable to calculate the distance around the Peninsula, so ice extent shapefiles were clipped to exclude the Weddell Sea region for the first few weeks to avoid miscalculating the true distance to the closest sea ice edge.

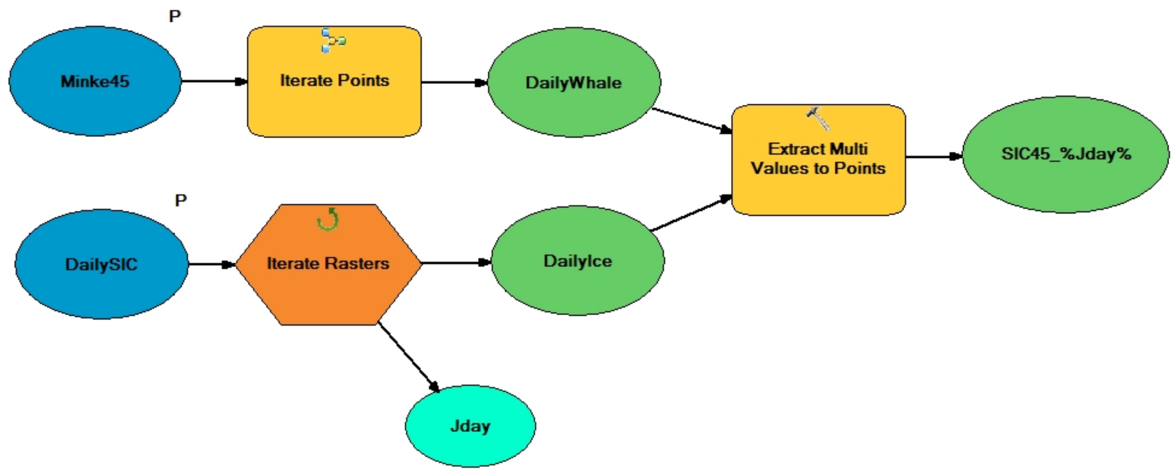

Figure 3.5: Schematic of ArcGIS ModelBuilder used to determine sea ice concentration.

3.4 Additional Environmental Data

Gridded environmental data, such as sea ice concentration, sea surface temperature, and bathymetry, were also evaluated using ArcGIS ModelBuilder. Figure 3.5 shows a schematic of the model used to calculate sea ice concentration values for each point in the whale data. The model iterates through both the daily sea ice concentration raster grids and the whale location data, matching the Julian days with the satellite tag timestamps. The *Extract Multi Values to Points* tool was used to extract cell values at each whale location and record the values in the attribute table of the input point feature class. The same model was used to obtain daily sea surface temperatures at each point by replacing the DailySIC parameter with DailySST. Since bathymetry is a temporally static dataset, the *Extract Multi Values to Points* tool was applied to the entire track without iterating through Julian days.

3.5 Generalized Additive Models

Generalized additive models (GAMs) are used to determine the non-linear relationships between predictor and response variables. GAMs are a generalization of multiple regression in which the linear form is replaced by a sum of non-parametric smooth functions represented by penalized regression splines to achieve the best prediction of the dependent variable. Additive models are particularly advantageous in uncovering nonlinear covariate effects of the independent variables. In addition, generalized additive mixed models (GAMMs) are an extension of GAMs that include both fixed and random effects. This model is most useful in making inferences on the entire population from which individuals are randomly sampled. We can assume there will be some correlations between observations of the same individual, so GAMMs are used to investigate covariate effects on movement analysis.

GAMs allowed us to determine which set of environmental variables best predicts Antarctic minke whale foraging spaces around the Western Antarctic Peninsula. Feeding episodes were isolated from migrating behavior to more accurately evaluate the influence of dependent variables on foraging behavior. Similar to Postlethwaite et al. (2013), we defined foraging behavior as area-restricted movement with MSSI values less than 0.5. Therefore, each whales' track was truncated at the point at which their behavior switched from primarily area-restricted (foraging) to primarily transient (migrating). At this point, the whale was increasing its distance from the ice edge and their MSSI approached 1.0, or straight-line movement.

For each individual whale track, GAMs were fit with the *gamm4* package (Wood & Scheipl, 2014) in R with a Gaussian distribution. The *gamm4* package was also employed to fit GAMMs using the aggregate of all three whales' data, a Gaussian distribution, and a random effect term for individuality. Models were built using varying combinations of environmental variables with correlations less than 0.7 to reduce multicollinearity (Table 3.2). Two GAMs were generated for each whale; including all variables, and extracting only the distance to SIE variables. GAMMs were built on the aggregated whale data using the same set of variables. For each environmental covariate, we calculated the daily change in the environmental condition, which resulted in the change in SIE (ΔSIE), SST (ΔSST), and bathymetry (Δbath).

Finally, each model was also duplicated using a daily average of the environmental and MSSI conditions. The first GAMs modeled MSSI based on four

Table 3.2: Descriptions of each generalized additive model run. Generalized additive mixed models were utilized for the aggregated whale data to account for random effects of individuality. All models predicted the MSSI and used a Gaussian distribution. Abbreviations: Jday = Julian Day, lat = latitude, SIE = distance to the ice edge(km), ΔSIE = change in distance to the ice edge, SST = sea surface temperature(C), ΔSST = change in sea surface temperature, bath = bathymetry(km), Δbath = change in bathymetry, ID = tag ID.

Source Data	Model Formulation
112745	s(Jday)+s(lat)+s(SIE)+s(ΔSIE)+s(ΔSST)+s(Δbath)
	s(SIE)+s(ΔSIE)
112747	s(SIE)+s(ΔSIE)+s(SST)+s(ΔSST)+s(bath)+s(Δbath)
	s(SIE)+s(ΔSIE)
112750	s(lat)+s(SIE)+s(ΔSIE)+s(SST)+s(ΔSST)+s(bath)+s(Δbath)
	s(SIE)+s(ΔSIE)
Three whales	s(Jday)+s(lat)+s(SIE)+s(ΔSIE)+s(ΔSST)+ random = ID
	s(SIE)+s(ΔSIE)+ random = ID

locations per day, every six hours. This method, however, introduced pseudo-replication due to the comparison of four points to a single, daily environmental remotely sensed image. Therefore, environmental and MSSI conditions were averaged per day and the deltas were recalculated, resulting in the two final GAMs per data source that were preferentially analyzed and discussed further, as described in Table 3.2.

The Akaike Information Criteria (AIC) provided a measure for variable selection. This criterion compares models in order to identify the optimal and parsimonious model that explains the most variance with the least number of variables. A minimum AIC value is desired, so we considered models with ΔAIC <2.

3.5.1 Cross Validation

K-fold cross validation was used to evaluate how well the model performed. Cross validation is a better indicator of model performance than residuals because it evaluates the ability to make new predictions on untrained data. This method separates the data into two sets, known as the training and testing sets, where the model is applied to the training set and then used to predict output values based on the testing set. The error produced in predicting the testing set is accumulated to provide the mean absolute error, which is used to evaluate model performance. Cross validation is preferred over the residual method, yet the evaluation can result in high variance and may heavily depend on which data are present in the training and testing sets.

In order to correct for this dependence on where the data is divided, k-fold cross validation was used in this study. In k-folding, the data set is randomly separated into k subsets and cross validation is performed k times. Each time, one of the k subsets is used to test the model and the other k-1 subsets are combined and used as the training data. The variance of the resulting prediction decreases as k increases, yet due to the fact that the training algorithm must be applied k times, the computational time also increases. In this study, a k value of 5 was used, where the cross validation was run 5 times, each time using a different, randomly divided, subset of the data as the testing set while the other four subsets were used to train the model.

Chapter 4

RESULTS

4.1 Whale Movement

Each whales' tag remained active for between 109 and 180 days, transmitting the whales' locations. During the first few weeks after the satellite tags were deployed, the three whales remained within Wilhelmina and the adjacent bays. On March 5th, Whale 1 departed the bays and traveled north, along the coast, toward the Drake Passage and Weddell Sea. Once north of the Peninsula, it paused for 3 days before traveling east into the Weddell Sea. Whale 1 spent the next two months north of the Weddell Sea between 60°S and 65°S. On May 22nd, Whale 1 migrated north of 60°S into the Scotia Sea before the tag detached on 29 May 2013.

Whale 2, however, departed the bays on February 21st and traveled south and west along the coast of the Peninsula before pausing for several days off the coast of Thurston Island, at approximately 99°W. This individual then slowly continued toward the Ross Sea. In mid-March, at approximately 145°W, it changed direction and headed back along the coast in a northeasterly direction. On April 25th, at approximately 116°W, Whale 2 changed its heading again, migrating north into the Pacific Ocean until the tag detached on 31 May 2013.

Whale 3 demonstrated much more area-restricted behavior, remaining in the bays for the majority of the tag's lifetime. As the season progressed, it moved into more southerly bays, but remained within 64°S and 67°S. At the end of May, Whale 3 departed the bays for several days before migrating north into the Pacific Ocean on June 8th. In more northerly waters of the Pacific Ocean, Whale 3 demonstrated interesting movement patterns north of 30°S, and seemed to be heading back toward

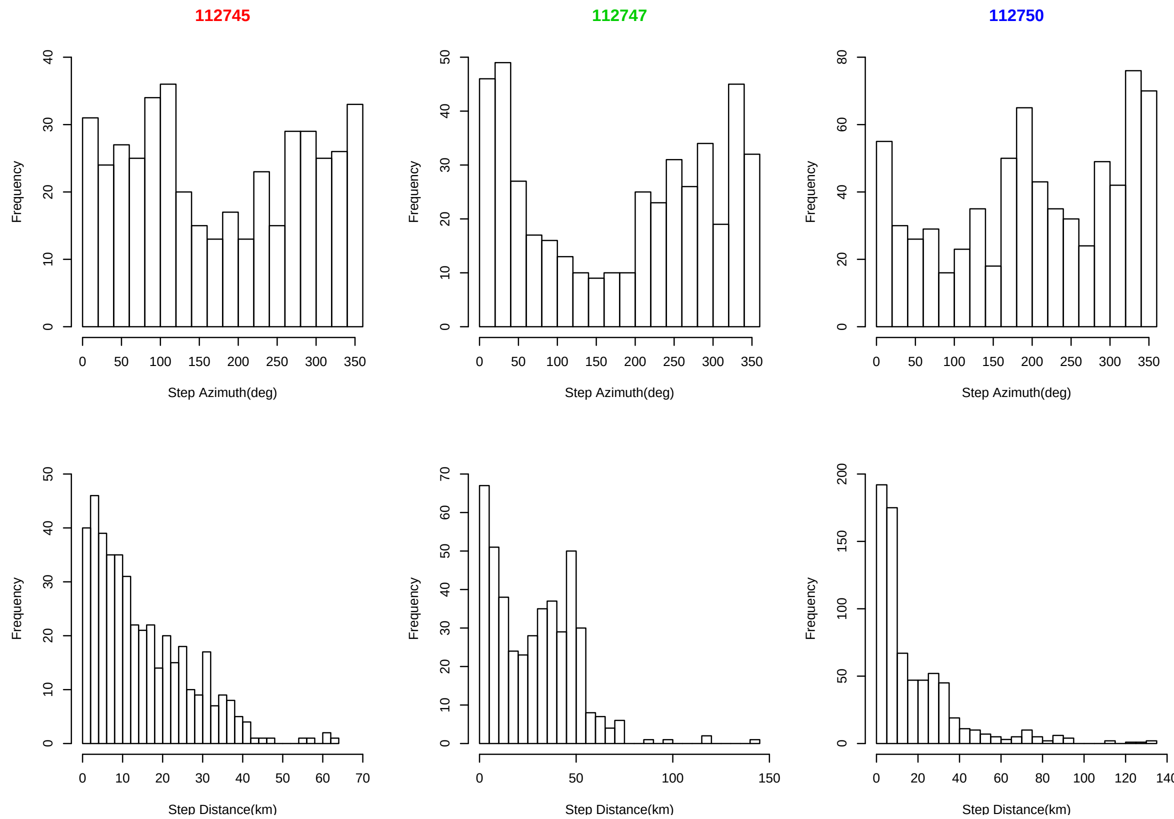

Figure 4.1: Daily step angle and step distance frequencies for individuals 112745, 112747, and 112750 throughout the lifespan of each satellite tag

the Southern Ocean in mid-July before the tag detached on 8 August 2013, but understanding the detail of this behavior in the tropics is beyond the scope of this project.

With approximately constant azimuth frequencies and heavily right-tailed distance frequencies (Figure 4.1), these three minke whales demonstrated at least two strong behavioral states, switching between periods of long distance, relatively straight, travel and periods of short distance, highly tortuous, movement. Whale 2's azimuth distribution, however, exhibited two preferred directions of travel, which correspond to it traveling west along the coast of Antarctica toward the Ross Sea and then returning east along the coast before heading into more northerly waters in the Pacific Ocean.

Table 4.1: Summary statistics of MSSI calculations for each individual (mean ± SD).

	112745	112747	112750
Total Track	0.40 ± 0.23	0.72 ± 0.26	0.44 ± 0.37
February	0.18 ± 0.14	0.55 ± 0.34	0.15 ± 0.06
March	0.46 ± 0.24	0.65 ± 0.19	0.18 ± 0.12
April	0.42 ± 0.18	0.73 ± 0.22	0.13 ± 0.13
May	0.49 ± 0.20	0.97 ± 0.03	0.26 ± 0.13
June	–	–	0.86 ± 0.16
July	–	–	0.94 ± 0.05
August	–	–	0.97 ± 0.01

Periods of area-restricted behavior, quantified by MSSI values close to zero, have been interpreted as demonstrating resting or foraging behavior, whereas periods of relatively straight tracks, quantified by MSSI values close to 1, suggest oriented movement such as migratory behavior, with 0.5 declared at the cutoff point (Postlethwaite et al., 2013). Individually, each whale in this study exhibited different patterns of behavioral states throughout the lifetime of each satellite tag (Figure 4.2). While in the bays of the Western Antarctic Peninsula, however, all three whales demonstrated highly tortuous tracks then transitioned into more oriented movement as the season progressed (Figure 4.3, Table 4.1). This change in movement patterns demonstrates a transition between foraging and transiting behavior, indicating a particular foraging season for these three individuals. Whale 1 exhibited the most frequent switches between behavioral states, spending 58% of its time foraging or resting. Whale 2, however, preferred traveling in a more straight-line trajectory, with only 16% more tortuous behavior. Finally, Whale 3's track was highly tortuous between February and May, before switching to a more migratory behavioral state between June and August. Overall, Whale 3 exhibited higher tortuosity for 63% of its total track length.

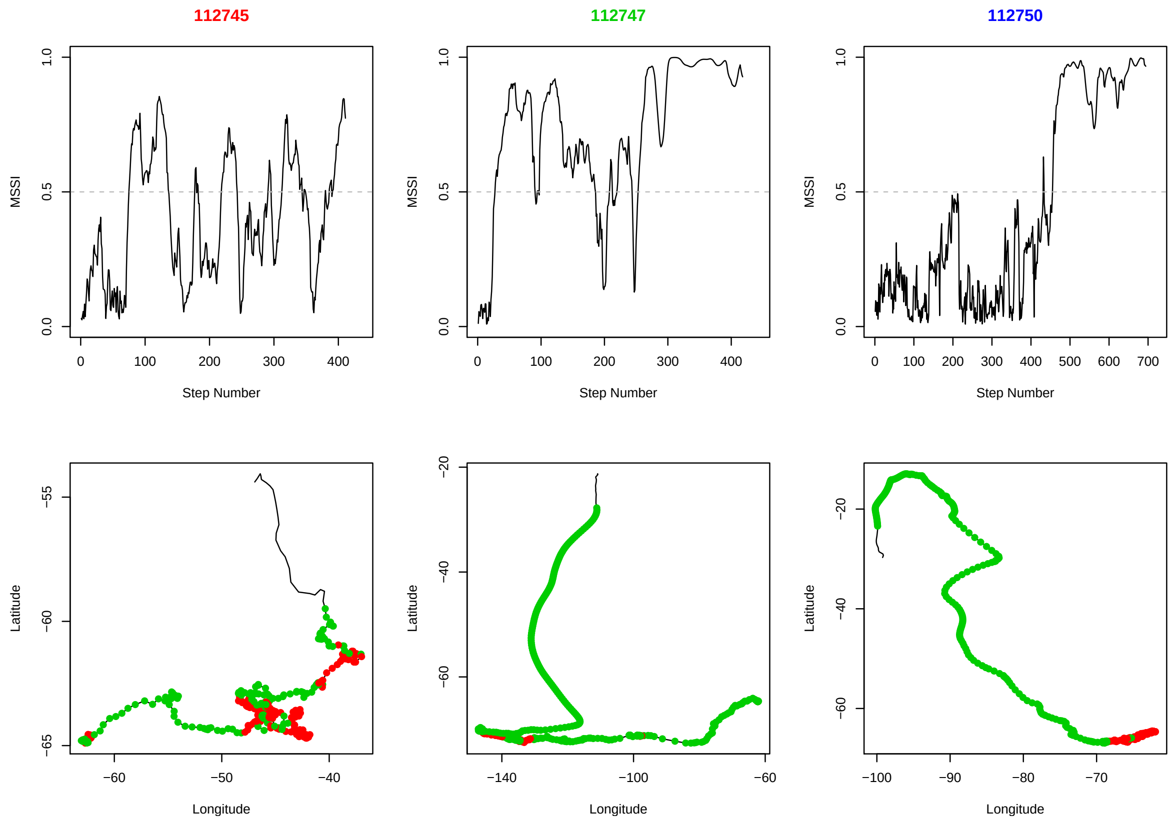

Figure 4.2: Results of the MSSI computation over each individual's entire track length. The first row shows the MSSI over time and the second row shows the trajectory data in spatial coordinates with points colored according to approximate behavioral states, where green are MSSI values >0.5 (migrating) and red are MSSI values $\leq$ 0.5 (foraging). Colored points are absent from the terminus of each track because they do not contain MSSI values due to the window size restrictions.

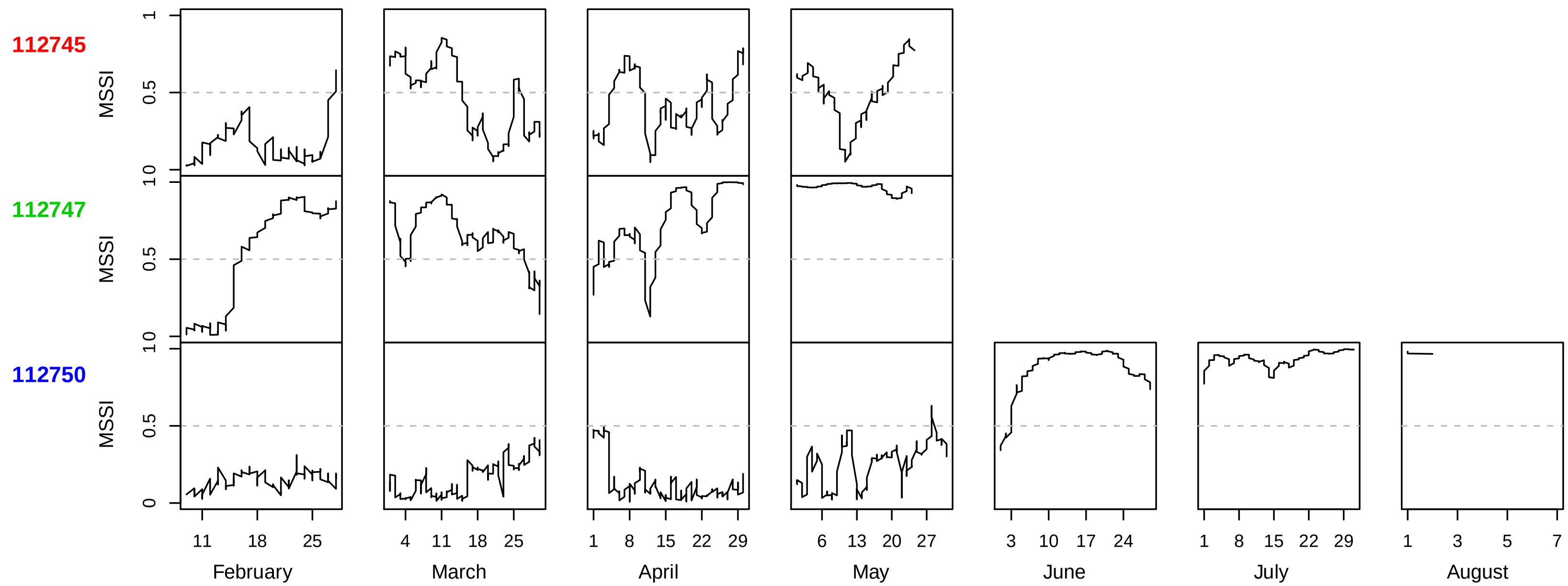

Figure 4.3: Monthly changes in MSSI across each whales' entire track length, where MSSI values >0.5 indicate transiting behavior and MSSI values ≤ 0.5 indicate foraging behavior. The tags on whales 112745 and 112747 detached in May, while 112750's tag remained attached until August.

4.2 Environmental Preferences

The whales' tracks were truncated before their northward migration to isolate their preferred environmental conditions with respect to foraging spaces (Figure 4.4). The end of the foraging season was defined according to successively increasing distance from the sea ice edge and MSSI values approaching 1.0 (Figure 4.5). The tracks were truncated on May 22nd, April 25th, and June 8th for Whale 1, 2, and 3, respectively. During this time, when the whales were considered in a primarily area-restricted and foraging state, environmental conditions were evaluated in order to characterize their foraging habitat preferences.

The three whales exhibited different habitat preferences with respect to local sea ice conditions (Figure 4.6). For most of the study period, Whale 1 remained within the marginal ice zone in ice concentrations greater than 50%. This individual spent the majority of its time north and east of the Antarctic Peninsula and in the Drake Passage. Whale 2 followed the coastline and SIE as it traveled through the Bellinghausen and Amundsen Seas, predominantly within 50 km of the SIE, before traveling north into the Pacific Ocean. This whale preferred low SIC until approximately mid-March when it started moving in and out of higher concentrations. Whale 3 preferred the bays of the Western Antarctic Peninsula (WAP), remaining close to the SIE and in low SIC. Whale 1 exhibited a bimodal distribution of SIC values, preferring low concentrations in the first few weeks and moving into higher concentrations later in the season, whereas Whales 2 and 3 preferred lower concentrations throughout the study period.

Due to its coarse temporal resolution (biweekly), sea ice thickness was not correlated to the daily movements of the whales. However, using the centroid location of each two week period, we summarized the whales' preference in sea ice thickness. Over the course of the study period, each whale demonstrated a habitat shift in ice thickness coincident with its shift in sea ice concentration and distance to the ice edge. When the whales were observed deeper in the ice pack, they encountered ice as thick as 1.5 m. Whale 1, in particular, preferred pack ice habitat far from the ice

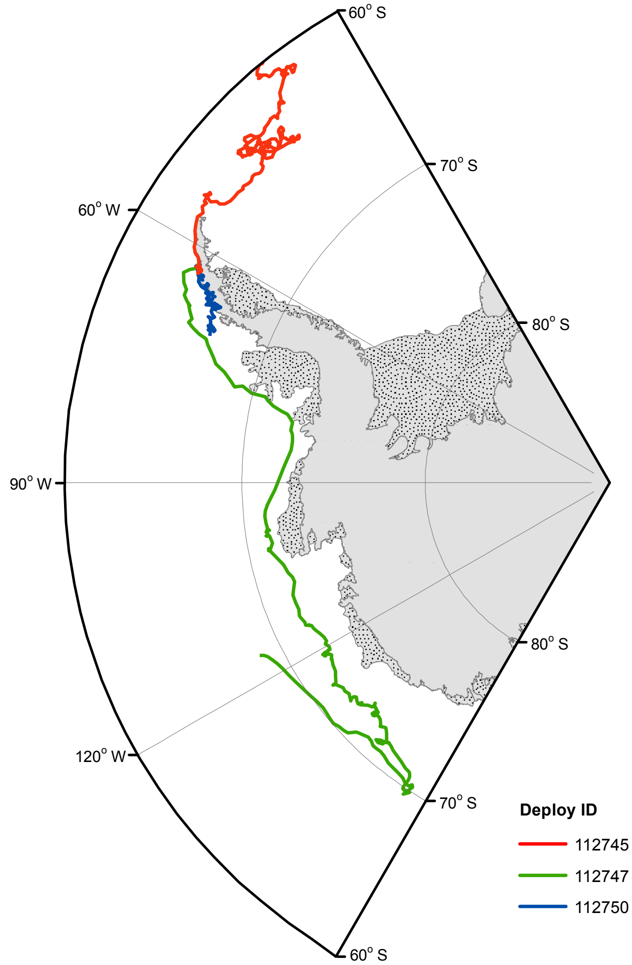

Figure 4.4: Whale tracks truncated before northward migration.

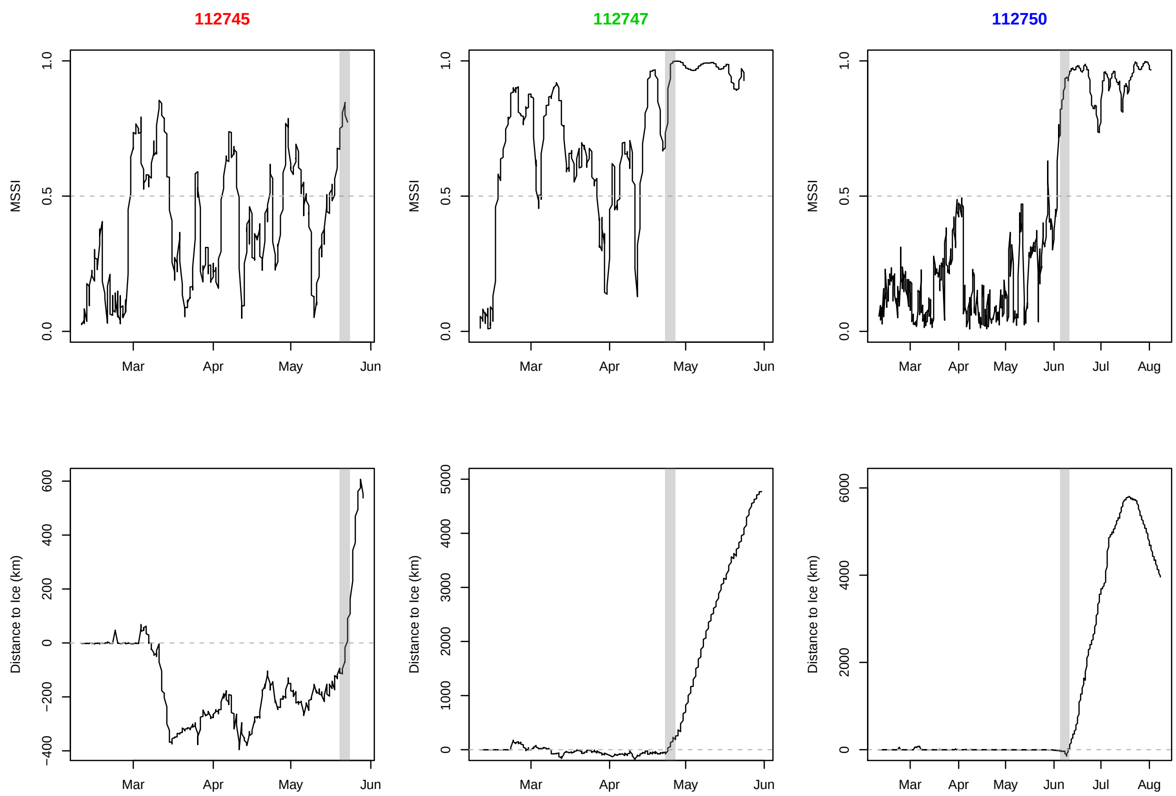

Figure 4.5: Point of data truncation defined by behavior switching from primarily space-restricted to primarily transient, as seen by MSSI approaching 1.0, and increasing distance from the sea ice edge. Negative distance to the ice edge values indicate distance calculated from within the ice pack.

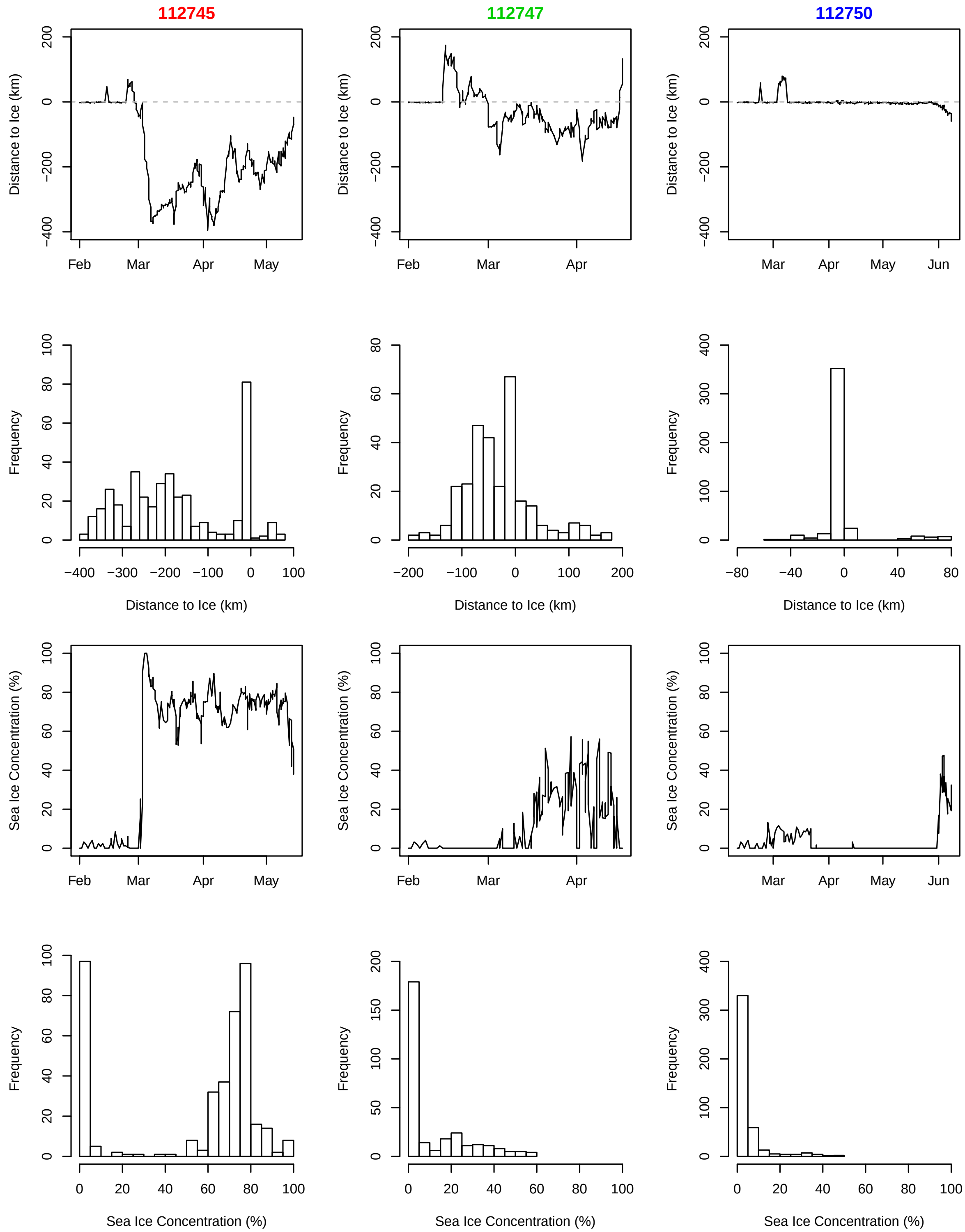

Figure 4.6: Daily sea ice conditions for each individual during the foraging season with frequency distributions. Negative distance to the ice edge values indicate distance calculated from within the ice pack.

edge, in higher concentrations and thicker ice. Whales 2 and 3, however, preferred ice thinner than 1.0 and 0.6 m, respectively. These preferences correspond to their individual choice in sea ice concentration and distance to the ice edge.

These whales also demonstrated habitat preferences with respect to bathymetry and sea surface temperature (SST) (Figure 4.7). During this study period, each whale preferred to remain on the continental shelf, in waters 500 m or shallower. Whales 1 and 2 demonstrated bimodal distributions of water depths, preferring shallow waters early in the season before moving into deeper water as the season progressed. Whale 3, however, remained in shallow water, less than 1 km deep, for the duration of the foraging season. Each individual preferred negative SSTs, coinciding with their preference for sea ice habitat, but while in the bays of the WAP during the austral summer, they were more likely to be exposed to positive SSTs.

In order to test for significant changes in habitat preference, change point analysis and Mann-Whitney U-Tests were performed. Mann-Whitney U-Tests were chosen because the data were not normally distributed. With respect to each of the four environmental variables (distance to SIE, SIC, bathymetry, and SST) the three whales demonstrated the same change in behavior with regards to the direction of habitat change, yet the magnitude and timing differed (Figure 4.8, Table 4.2). Each of these habitat shifts was statistically significant at an alpha level of 0.01. The majority of habitat shifts took place between late February and early March, with two exceptions: Whale 3 experienced the most significant change in SST on June 1st and did not significantly change its bathymetric preference throughout the feeding season, instead preferring the shallower waters of the continental shelf. For each individual, distance to SIE decreased to negative values in early March, indicating a shift from open water to sea ice habitat. This preference for pack ice habitat is also evident in their movement to higher ice concentrations (Figure 4.8). Whales 1 and 2 remained in the shallow waters of the continental shelf, ($<$500 m), until mid-March when they moved into significantly deeper waters, approximately 3.5 km (Table 4.2). Finally, each whale experienced a negative shift in sea surface temperature. Whale 1 and 2's

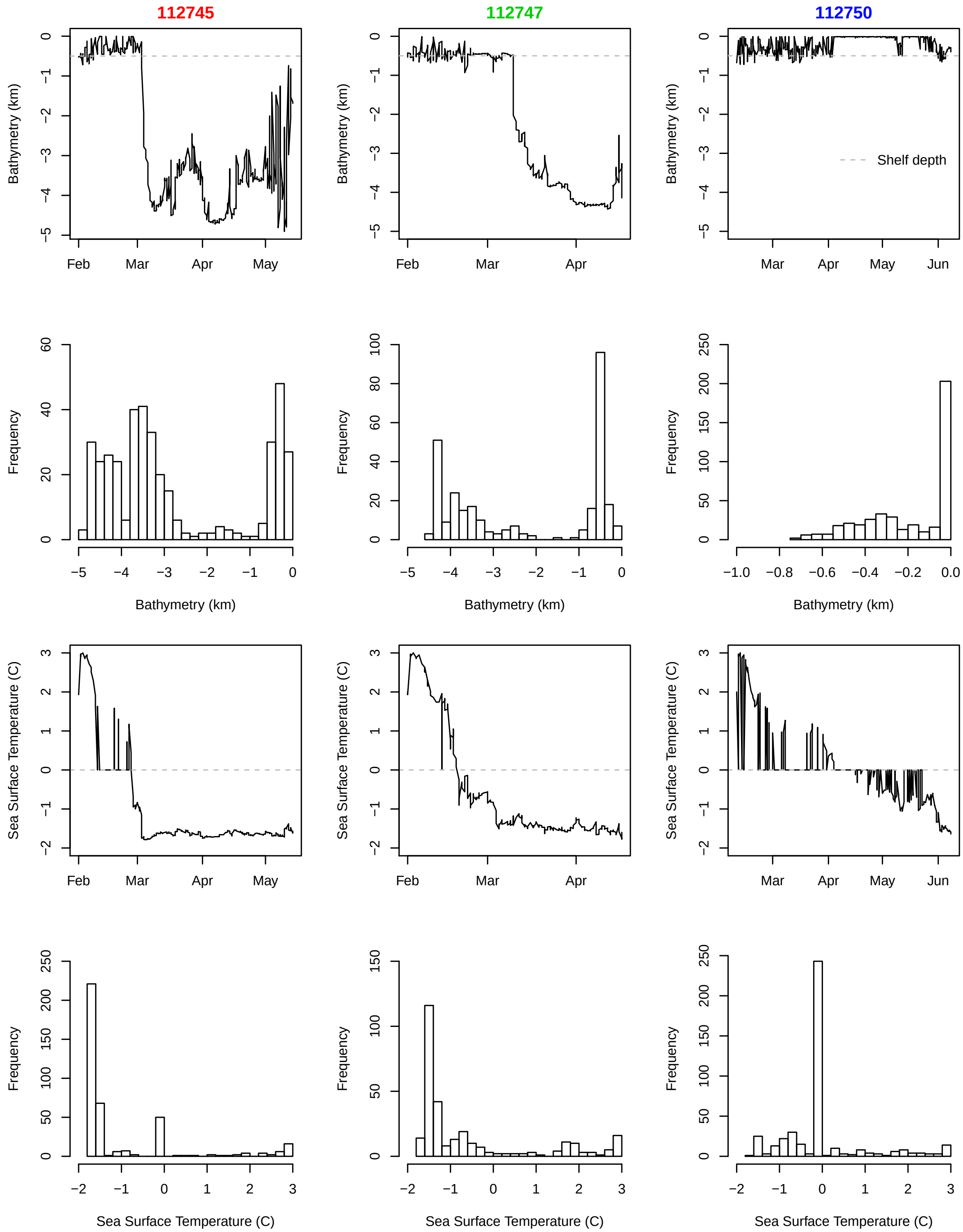

Figure 4.7: Daily sea surface temperature and bathymetric conditions for each individual with frequency distributions during the foraging season.

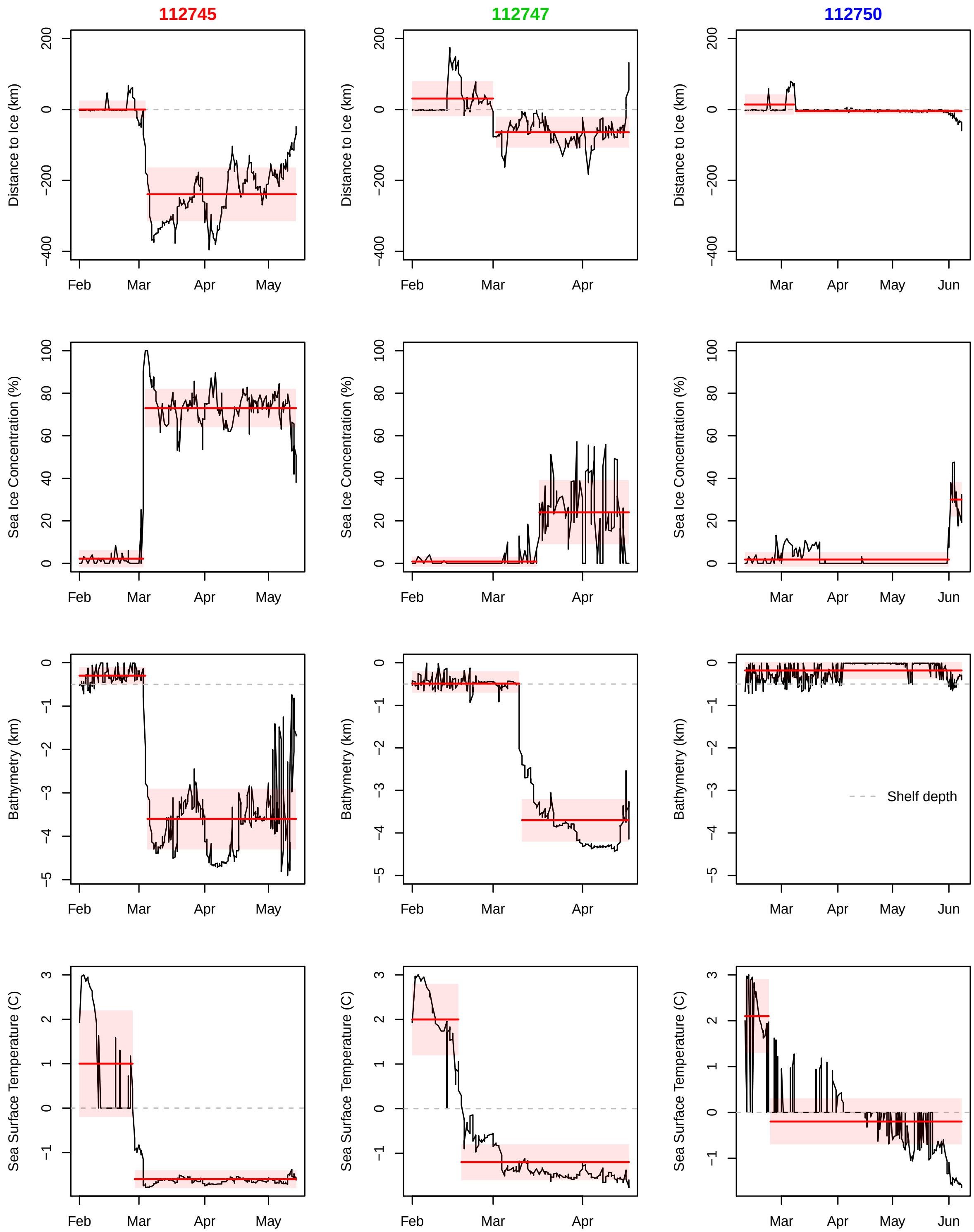

Figure 4.8: Dates of significant change in habitat preference. Red bars indicate average values for the period before and after the date of most significant habitat change with shading indicating ± 1 standard deviation. Dates of habitat change and mean values are reported in Table 4.2.

Table 4.2: Summary statistics of change point analysis using Mann-Whitney U-Tests with statistically significant results in bold.

			Before		After			
		Date	n	Mean ± SD	n	Mean ± SD	Z-score	p-value
112745	SIE(km)	12 March	110	-0.42 ± 25.21	286	-239.26 ± 75.51	15.41	**<2.2e-16**
	SIC(%)	11 March	106	2.20 ± 4.28	290	73.77 ± 9.09	-15.24	**<2.2e-16**
	Bath.(km)	12 March	110	-0.33 ± 0.23	286	-3.66 ± 0.77	15.40	**<2.2e-16**
	SST(C)	6 March	91	1.04 ± 1.26	305	-1.61 ± 0.17	14.48	**<2.2e-16**
112747	SIE(km)	9 March	106	30.95 ± 49.15	191	-64.08 ± 43.90	13.46	**<2.2e-16**
	SIC(%)	24 March	169	0.85 ± 2.41	128	24.08 ± 15.80	-11.84	**<2.2e-16**
	Bath.(km)	18 March	145	-0.50 ± 0.22	152	-3.77 ± 0.58	14.90	**<2.2e-16**
	SST(C)	25 February	62	2.04 ± 0.76	235	-1.25 ± 0.42	12.10	**<2.2e-16**
112750	SIE(km)	8 March	97	14.40 ± 28.18	332	-4.55 ± 7.47	8.63	**<2.2e-16**
	SIC(%)	1 June	403	1.90 ± 3.47	26	30.25 ± 8.46	-8.55	**<2.2e-16**
	Bath.(km)	-	-	-	-	-	-	-
	SST(C)	22 February	46	2.13 ± 0.87	383	-0.21 ± 0.57	10.15	**<2.2e-16**

temperature shifts coincided with their shifts in ice conditions, and therefore indicates an intentional habitat change. Whale 3's temperature shift, however, occurred earlier than significant changes in sea ice conditions, which may be indicative of a preference for the location of the WAP bays and not specific environmental conditions. The significant change in Whale 3's distance to SIE is a result of the unusually low ice extent between March 4^{th} and 8^{th}, and not an intentional migration farther from the pack ice. Instead of traveling into open water, this individual remained in the same bay south of Wilhelmina Bay during this fluctuation in ice concentration.

Significant differences were also detected between migrating and foraging behaviors, as defined by the MSSI (Table 4.3). Whale 1 demonstrated a greater negative distance to the sea ice edge during foraging bouts, indicating a preference for pack ice habitat, as well as as preference for shallower depths and slightly warmer waters. Whale 2 also significantly preferred dense pack ice habitat as seen by a greater negative distance from the ice edge and greater sea ice concentration during foraging and resting behavioral states. Whale 3, however, preferred foraging in less dense ice packs, while also remaining in the shallower and warmer waters of the WAP bays.

4.3 Model Predictions

Each model run is documented in Table 4.4 with dependant variables, R^2, ΔAIC, and area under the curve (AUC) before and after k-fold cross validation. The AUC is calculated from the receiver operating characteristic (ROC) curve and is a commonly-used method for validating model performance. The GAM models here exhibit little change in the AUC before and after k-fold cross validation was performed and therefore demonstrate sufficient model performance. Model selection was based on the ΔAIC and R^2, so the models built on all covariates, instead of only sea ice extent variables, were the most parsimonious.

Using generalized additive models (GAMs), we found that each model had a different set of covariates, minimizing the effects of multicollinearity. Two covariates,

Table 4.3: Differences in foraging and migrating habitat preferences using Mann-Whitney U-Tests with statistically significant results in bold.

		Foraging	Migrating	Z-score	p-value
112745	n	246	150		
	SIC(%) (mean±SD)	54.45 ± 32.27	54.88 ± 33.60	0.34	0.73
	SIE(km)	-194.58 ± 131.70	-137.19 ± 106.17	4.83	**1.36e-06**
	Bath.(km)	-2.91 ± 1.65	-2465 ± 1.58	3.77	**0.00016**
	SST(C)	-0.84 ± 1.50	-1.26 ± 0.73	-2.01	**0.04**
112747	n	68	229		
	SIC(%)	17.67 ± 17.45	8.84 ± 14.43	-4.82	**1.57e-76**
	SIE(km)	-52.25 ± 54.57	-23.61 ± 65.99	2.66	**0.0079**
	Bath.(km)	-2.34 ± 1.71	-2.12 ± 1.70	0.43	0.66
	SST(C)	0.12 ± 2.05	-0.77 ± 1.11	-1.08	0.28
112750	n	407	22		
	SIC(%)	2.40 ± 5.04	26.16 ± 11.99	6.81	**4.08e-16**
	SIE(km)	1.19 ± 15.77	-27.07 ± 13.71	-6.99	**2.71e-12**
	Bath.(km)	-0.18 ± 0.20	-0.38 ± 0.15	-4.21	**2.17e-05**
	SST(C)	0.12 ± 0.90	-1.46 ± 0.22	-7.61	**2.20e-16**

Table 4.4: Description of generalized additive models with ΔAIC, R^2, and AUC before and after k-fold cross validation. All models predicted the MSSI and used a Gaussian distribution. The second model for each source data predicted the MSSI using only distance to the sea ice extent variables. Model formulations are listed in Table 3.2.

Source Data	R^2	ΔAIC	AUC before	AUC after
All Whales	0.371	0	0.8078	0.8236
All Whales ice	0.166	209	0.5730	0.4493
112745	0.515	0	0.9577	0.8637
112745 ice	0.160	50	0.7554	0.6813
112747	0.591	0	0.8856	0.7892
112747 ice	0.057	57.1	0.6356	0.5932
112750	0.795	0	0.9896	0.9805
112750 ice	0.571	447.5	0.9130	0.9013

distance to sea ice edge (SIE) and change in distance to sea ice edge (ΔSIE), were included in each model run, yet only SIE had a significant influence on the MSSI for each run at the 0.05 or less significance level. Change in sea surface temperature (ΔSST) was included in all models, excluding ice-only model runs, yet was only significant in whale 1's environmental model (p=0.001). For each model in which it was included, SST exhibited significant influence on the MSSI at the 0.05 or less significance level, however, Δbath was only significantly influential to whale 1's model (p=0.001). Bathymetry (bath) was only included in 2 of the model runs, but only significantly influenced whale 2's model.

Response curves and reported statistics for each model run are provided in Appendix A. Generalized additive mixed models built on the aggregation of the three whales' tracks demonstrated strong relationships with SIE, ΔSIE, and SST (Figure A.1). The MSSI was predicted to be closer to 0 for these three individuals when they were at least 50 km inside the ice pack, moving back toward the ice edge, and in positive SSTs. Although date (Jday) and latitude were statistically significant (p=0.01 and p=0.05, respectively), their response curves remained approximately constant around the MSSI's mean and were therefore not ecologically interpretable (Figure A.1.a and A.1.b). ΔSST demonstrated no significance and a horizontal response curve, indicating no influence on the predictor variable (Figure A.1.f).

Whale 1's GAM exhibited positive relationships with latitude and SIE, a negative relationship with Δbath, and a bimodal relationship with date (Figure A.3). These variables predicted low MSSI during February and May, south of 63°S, at least 150 km within the ice pack, and while the whale moved into shallower waters. ΔSIE and ΔSST showed little influence on the MSSI (Figure A.3.d and A.3.e).

Whale 2's GAM showed strong relationships with SIE, SST, and bathymetry, while ΔSIE, ΔSST, and Δbath showed little to no relationship with the MSSI (Figure A.5). This individual's MSSI was predicted to be closer to 0 when it was at least 50 km inside the marginal ice zone, in warmer waters, and between 2.5 and 4 km water column depth.

Whale 3's GAM was most strongly influenced by the SIE (Figure A.7.b). Low MSSI was predicted when this individual was outside the ice pack, up to 70 km from the sea ice edge. There was also a slight relationship with latitude and SST, where low MSSI was predicted around 65°S and in positive SSTs (Figure A.7).

Variable importance was also calculated for each model run (Figure 4.9). Distance to the sea ice extent was the only variable that was significantly important for each model run. Sea surface temperature was most influential for the aggregate of the three whales' data and for Whale 2, whereas latitude was only important for Whale 1 and Whale 3.

Finally, we tested the use of the change points analysis results in the GAM analysis. By treating the date of most significant habitat change as a factor variable (coded as 0 before the change and 1 after the change) for distance to the sea ice extent, sea surface temperature, and bathymetry, we were able to add these state shifts into the GAMs. Since these habitat shifts often took place at similar times, a few of these factor variables exhibited correlations >0.7 and were removed. After testing different combinations of uncorrelated factor variables on the generalized additive mixed model for all three whales' data, the shift in bathymetric conditions resulted in the best performing model based on the AIC (ΔAIC = -6). The MSSI was significantly influenced by the bathymetric shift (coefficient = -0.281, $p<0.001$), indicating the whales were more likely to exhibit foraging behavior before the date of most significant change in water depth. This result may be skewed by whale 3 since it did not demonstrate a state shift in bathymetric conditions, instead remaining in areas <500m deep and demonstrating highly tortuous movements.

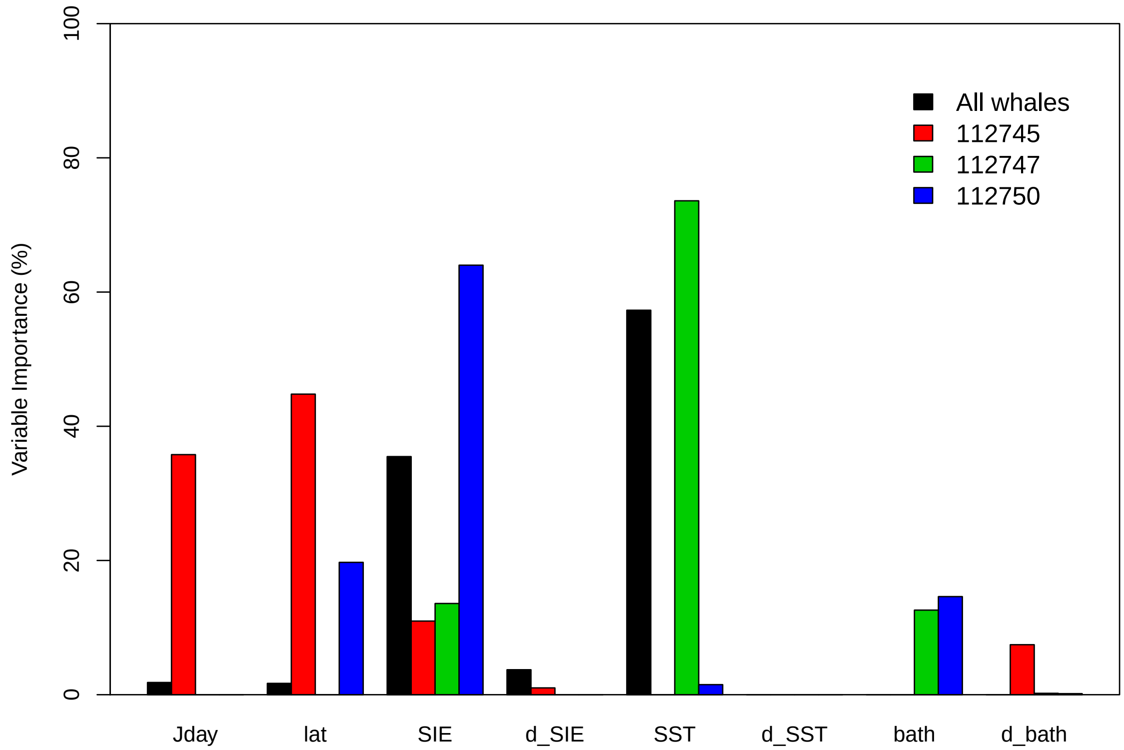

Figure 4.9: Relative variable importance for each generalized additive model run, excluding ice-only models. Columns labeled as d_SIE, d_SST, and d_bath represent the Δ variables.

Chapter 5

DISCUSSION

5.1 Reliability of Model Performance

The results of this study provide the first satellite tag-based analysis of Antarctic minke whale movement and habitat preference around the Western Antarctic Peninsula (WAP). Although the sample size is small, with only three individuals, the information gained from their tracks provides support for their pagophilic nature and identifies key environmental factors for predicting ideal foraging spaces.

The Multi-Scale Straightness Index (MSSI) developed by Postlethwaite et al. (2013) was used to evaluate the whales' movement patterns and ascertain changes in behavioral states throughout the length of the tracks. Due to their relatively small size, Antarctic minke whales demonstrate a smaller engulfment capacity while foraging compared to larger rorqual species such as humpback and blue whales (Goldbogen et al., 2012). A smaller engulfment capacity is directly related to higher lunge frequencies of short and small feeding bouts (Friedlaender et al., 2014; Goldbogen et al., 2012). The temporal resolution of this dataset restricts the ability of the MSSI to capture all foraging bouts. However, it can provide an understanding of the predominant behavior over a period of a few days. Friedlaender et al. (2014) directly observed Antarctic minke whales mostly foraging over a period of 18 hours, which suggests our daily MSSI behavioral states are indicative of the whales' primary behavior on a daily scale.

Generalized additive models (GAMs) were employed to identify correlations between environmental covariates and the computed values of the MSSI, providing a method for describing Antarctic minke whale foraging spaces. The major limitation of GAMs is the flexibility of the model, which has the potential to overfit the data. In order to account for this flexibility, covariates were assessed and removed if the model's Akaike Information Criteria (AIC) decreased by at least 2 after excluding that variable, indicating an improvement on model performance. GAMs can also be vastly improved by using *in situ* data or remotely sensed data with high spatial and temporal resolution.

Given the limited temporal resolution of the track data (6 hours) and spatial resolution of satellite-derived environmental data (approximately 50 m to 25 km) in these models, we believe the reliability of our model performance is satisfactory for gaining a better understanding of Antarctic minke whale movements over their foraging season and their habitat preferences with respect to sea ice dynamics.

5.2 Ecological Importance

The Southern Ocean's cold, nutrient rich waters support large stocks of krill, which attracts top predators that predominantly forage on euphausiids, such as sea birds, seals, and whales (Friedlaender et al., 2009; Laws, 1977). The Antarctic minke whale is a highly abundant cetacean in the region (Laws, 1977), and with its relatively compact body and high feeding rates, it plays a vital role in the dynamic and ecologically rich polar marine habitat of the Southern Ocean and Western Antarctic Peninsula (WAP).

5.2.1 Association with Sea Ice

As a pagophilic species, Antarctic minke whales have been observed in sea ice covered areas around Antarctica (Ainley et al., 2007; Scheidat et al., 2011). This species is perfectly adapted to exploit pack ice habitat as evidenced by their slim, compact body and small fins that allow for greater maneuverability in narrow passages between ice flows. Ribic et al. (1991) observed significantly more minke whales in the marginal ice zone (MIZ), characterized by new ice and pancake ice less than 0.10 m thick. Their hard, pointed rostrum also allows these whales to break through thin, young ice in order to breathe (Ainley et al., 2007; Bannister, 2002). Ainley et al. (2007) reported the MIZ was the best predictor of Antarctic minke whale sightings, with a higher probability of presence farther into the pack ice. Our results show these three individuals preferred habitat within the MIZ or in heavily sea ice covered areas during the foraging season, with 43% of the observations within 10 km south of the sea ice edge and 89% of the observations within the pack ice as opposed to open water, quantifying previously indirect observations. As the whales travel deeper into the ice pack, potentially hunting krill or avoiding Orca predation (Pitman & Durban, 2012), they punch breathing holes into the ice with their rostrums (Tynan et al., 2009). These holes also allow other polar marine predators, such as seals and penguins, to forage farther into the pack ice, providing an ecological service to other air-breathing marine species within the MIZ (Ainley et al., 2007; Tynan et al., 2009).

Interspecies resource partitioning and opposing spatial distributions, however, have been observed between humpback and minke whales in the Southern Ocean (Bombosch et al., 2014; Friedlaender et al., 2011, 2009). Even though both species remained near the coastline, minke whales seem to prefer colder, deeper waters while humpback whales were associated with increased krill biomass in the upper portion of the water column (Friedlaender et al., 2009). Bombosch et al. (2014) predicted habitat suitabilities for each species and found that minke whale habitat occurred south of those for humpback whales, indicating minke whales' preference for sea ice covered habitat. Using our tracking data to understand this relationship between humpback and minke whales is beyond the scope of this project, but will be the focus of future work.

5.2.2 Association with Additional Environmental Factors

In addition to their preference for sea ice habitat, Antarctic minke whales have been associated with continental shelf areas (Ainley et al., 2007; Beekmans et al., 2010) and colder water temperatures (Bombosch et al., 2014; Ribic et al., 1991). Our results also indicate these whales prefer shallower depths and cooler temperatures, with over 50% of the observations located within the 500 m continental shelf and 80% of the tag locations within negative SSTs.

Beekmans et al. (2010) performed GAMs on Antarctic minke whale density in open water, and found that transition zones, such as the continental slope, sea ice extent, and the circumpolar current front were the most important covariates, although their study region differed from ours with respect to sea ice cover and bathymetric complex. Transition zones often exhibit enhanced productivity due to the upwelling and concentration of deep, nutrient rich waters, providing ideal habitat for primary production and higher trophic level species. Minke whales have been associated with regions south of the Antarctic circumpolar current (Ainley et al., 2007; Branch, 2006; Nicol et al., 2000) and on the shelf and shelf break (Beekmans et al., 2010; Bombosch et al., 2014; Friedlaender et al., 2006), which is consistent with our results (Figure 5.1). During their foraging season, these three whales remained south of the southern boundary of the Antarctic Circumpolar Current (sbACC)[1] (Figure 5.1). When the whales transitioned into a more migratory behavioral state, they crossed the sbACC and traveled north. With the exception of the latter portions of Whale 1 and 2's tracks, the three whales also remained on or around the continental shelf. Whale 2, in particular, remained on or near the 500 m continental break as it followed the ice edge along the coast between February and March, while the other two preferred shallower waters while they were adjacent to the continent (Figure 4.8).

During the beginning of the study period, in the austral summer (February and March), the waters around the WAP were relatively warm, particularly in the shallow bays. When Whales 1 and 2 left the bays, they transitioned into deeper, cooler waters (Figure 4.8). Whale 3, however, remained in the bays for the entire study period, traveling to progressively more southerly bays as the season progressed.

[1] http://gcmd.nasa.gov/records/AADC_southern_ocean_fronts.html

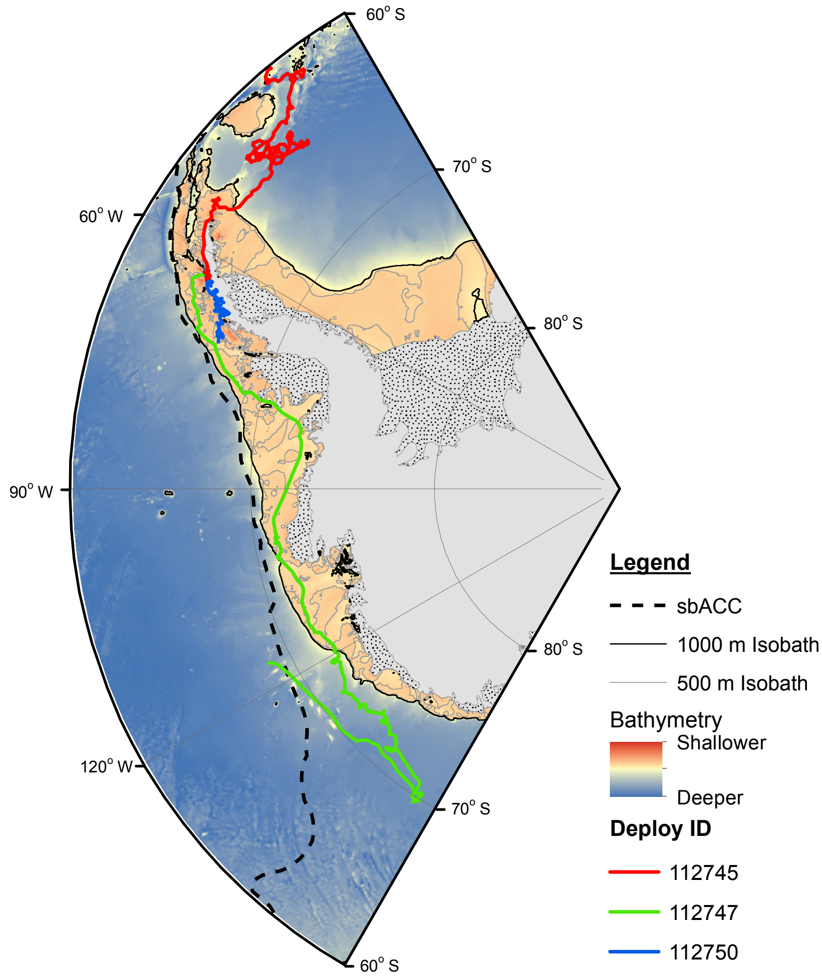

Figure 5.1: Minke whale tracks with bathymetric contours and the southern boundary of the Antarctic Circumpolar Current (sbACC).

Although Ribic et al. (1991) and Kasamatsu et al. (2000) observed a significantly negative relationship between SST and minke whale density, SST alone could not explain minke whale density and must instead be considered with other environmental factors, such as water column depth and prey aggregations.

The association of minke whales with sea ice, cooler waters, the sbACC, and the shelf break is likely due to high prey abundances, particularly Antarctic krill (*Euphausia superba*) and ice krill (*Euphausia crystallorophias*) (Tynan et al., 2009). Sea ice provides a surface on which algal communities can flourish suspended in the upper portion of the water column, where light can penetrate for photosynthesis (Arrigo et al., 2009). Sea ice algae, in particular, are the primary food source that supports higher trophic level species in the polar ocean such as krill, penguins, seals, and whales (Arrigo et al., 2009). Our results indicate that minke whales prefer to remain along the edge of the sea ice as well as farther into the marginal ice zone, likely attracted by the dense krill aggregations that prefer the shelf break, in the cool, nutrient rich waters south of the sbACC (Nicol, 2006).

5.3 Identifying Foraging Spaces

Antarctic minke whales are known to consume Antarctic krill (*Euphausia superba*) and ice krill (*Euphausia crystallorophias*) (Tynan et al., 2009). High densities of minke whales have been observed along the sea ice edge and on the continental shelf due to dense prey aggregations along these transition zones (Murase et al., 2013). Results from GAM analysis performed in this study indicate these three minke whales demonstrated highly tortuous (interpreted as resting or foraging) behavior inside the ice pack and in slightly warmer surface waters (Figure A.1). This seemingly contradictory response between warm waters and pack ice habitat may be an artifact of the data. Undetected sea ice is known to cause unrealistically warm optimally interpolated sea surface temperatures (OISST), particularly near the ice edge where the ice is patchy and not fully solidified. These areas are ideal foraging locations for Antarctic minke whales, which may cause discrepancies between our results and those of previous research.

The tags were deployed in February, during the annual minimum sea ice extent at the end of the austral summer, when waters surrounding the WAP were warmer with thin, patchy sea ice. Summer foraging near the sea ice extent, therefore, can be characterized by sea ice concentrations of $<10\%$, surface temperatures of $\pm 1°C$, and water column depths of <500 m. As the season progressed, and the sea ice advanced, these minke whales were demonstrating foraging behavior farther into the ice as well as in cooler and deeper waters.

Chapter 6

CONCLUSIONS

6.1 Summary of Main Findings

This study provides the first satellite tag-based habitat analysis of Antarctic minke whales in the Southern Ocean around the Western Antarctic Peninsula (WAP). Little is known about the daily movements of minke whales, particularly because they tend to prefer sea ice habitat, where ship observations are restricted and the availability of icebreaker-supported helicopters is limited. Due to these restrictions, the pagophilic nature hypothesis has not been rigorously tested and direct correlations between daily movements and environmental factors have not been analyzed. In order to address these challenges, this study used ARGOS-enabled Spot-5 satellite tags to record the daily locations of three Antarctic minke whales during the foraging season, between February and May, as well as satellite-derived environmental data to correlate to the whales' movements.

As a pagophilic mesopredator, the Antarctic minke whale plays a vital role in the ecosystem of the Antarctic pack ice. With their slim, compact bodies, small fins and hard, pointed rostrums, Antarctic minke whales are well-suited to exploit prey aggregations within the marginal ice zone. Results from this study confirm their pagophilic nature. GAM analysis revealed that environmental conditions are the best covariates to predict minke whale foraging locations. These three individuals remained in the pack ice as opposed to open water for 89% of the study period and in ice concentrations of at least 20% for 34% of the time (Table 6.1). They also preferred to be on or near the continental shelf break and in waters of ± 1°C. Individual differences in environmental preferences were also evident and are recorded

Table 6.1: Percentage of whale locations observed in pack ice as opposed to open water, within at least 10km south of the sea ice extent (SIE), in sea ice concentrations (SIC) of at least 20%, in sea surface temperatures (SST) of ±1°C, and in continental shelf waters of 500m or less.

	All Whales	112745	112747	112750
Inside pack ice	89%	95%	79%	91%
At least 10km south of SIE	46%	21%	19%	86%
SIC of at least 20%	34%	72%	27%	5%
SST between -1 and +1°C	45%	20%	21%	81%
Water column depth <500m	57%	27%	33%	97%

in Table 6.1. Model results indicate ideal minke whale foraging habitat in the austral summer and fall, between February and May, is within the marginal ice zone, close to the Antarctic coastline.

After their feeding season ended, two individuals migrated north into the tropical Pacific Ocean, while the third remained in the Southern Ocean within the Scotia Sea. Previous research has shown evidence that some of the population remains in the Southern Ocean throughout the year while others potentially migrate north during the winter (Ensor, 1989; Miyashita et al., 1995). These behaviors may be indicative of age and sex-dependent migration patterns, and will be of interest in future work.

6.2 Applications for Model Predictions

The predicted foraging spaces presented in this study represent the first satellite tag-based analysis of Antarctic minke whale habitat preferences around the WAP during the austral summer feeding season. Although the habitat models used in this study are restricted to understanding foraging behavior of only three individuals, the results reproduce known minke whale feeding areas and confirm their association with sea ice habitat. Our good model performance allows us to extrapolate these results to a number of applications such as planning tools for conservation and future research in the ecology of the WAP.

Evaluating this species' habitat preference and population dynamics are necessary for developing appropriate conservation and management practices of the Commission for the Conservation of Antarctic Marine Living Resources (CCAMLR) and the International Whaling Commission (IWC). CCAMLR is working with international researchers and conservation organizations to protect marine resources in the Southern Ocean, particularly krill populations. They are currently working toward defining a new, larger Marine Protected Area in the Western Antarctic Peninsula region in order to protect krill stocks and higher trophic order predators such as penguins, seals, and whales. This study will aid CCAMLR in understanding Antarctic minke whale foraging habitat, which has been largely unknown before this satellite tag-based analysis.

This species is also the subject of a contentious 'scientific' lethal sampling program undertaken by the Japanese Whale Research Program under Special Permit in the Antarctic (JARPA). JARPA claims its current self-imposed annual catch limit of 333 minke whales is sustainable. The past two population estimates of minke whales in the Southern Ocean drastically decreased from 720,000 in 1985-1990 to 515,000 in 1992-2003. Current population estimates are not yet available, and without an accurate understanding of their habitat preferences and foraging behavior, CCAMLR, the IWC, and JARPA can not fully evaluate the stability of the minke whale population in the Southern Ocean. The most humane and efficient method of acquiring such data would be to use extensive ship- and aerial-based surveys farther into the pack ice, long term satellite tracking, and biopsy darts.

Understanding the ecology and migration patterns of cetacean species in the Southern Ocean is vital for interpreting the impacts of global climate change on polar marine ecosystems. The coupled relationship between minke whales, krill, and sea ice suggests that these whales will be sensitive to changes in sea ice concentration, extent, and duration, making them particularly vulnerable to climate change. Over the past 40 years, the sea ice season in the Bellinghausen and Amundsen Seas has decreased by approximately 2 months, dramatically reducing thick ice floes, surfaces for sea ice algae to grow, and vital habitat for higher trophic level species to hunt. This rapidly warming region in the Southern Hemisphere provides an ideal model for understanding the implications of global climate change, and will dictate the necessity for international cooperation and future research objectives.

6.3 Future Work

Future work will utilize each individual's entire track length in order to gain a better understanding of these whales' migratory behavior. The movement patterns of the tagged minke whales from this study provides the first evidence that some portion of this population leaves Antarctic waters during the winter season.

We are also interested in comparing long term Antarctic minke whale movement patterns with the known movements of humpback whales in the Southern Ocean and migration to the tropics. In order to gain a wholesome understanding of Antarctic minke whales, additional tags will need to be deployed with a specific focus on winter behavior. It would also be advantageous to acquire additional information on each of the tagged individuals to study differences in age and sex-dependent behavior.

REFERENCES

Ainley, D. G., Dugger, K. M., Toniolo, V., & Gaffney, I. (2007). Cetacean occurrence patterns in the Amundsen and southern Bellingshausen sea sector, southern ocean. *Marine Mammal Science*, *23*(2), 287–305.

Ainley, D. G., Jongsomjit, D., Ballard, G., Thiele, D., Fraser, W. R., & Tynan, C. T. (2012). Modeling the relationship of Antarctic minke whales to major ocean boundaries. *Polar Biology*, *35*(2), 281–290.

Arnason, U., Gullberg, A., & Widegren, B. (1993). Cetacean mitochondrial DNA control region: sequences of all extant baleen whales and two sperm whale species. *Molecular biology and evolution*, *10*(5), 960–970.

Arrigo, K. R., Mock, T., & Lizotte, M. P. (2009). Primary producers and sea ice. In D. N. Thomas, & G. S. Dieckmann (Eds.) *Sea Ice*. Oxford: Wiley-Blackwell, 2nd ed.

Bannister, J. L. (2002). Baleen Whales Mysticetes. In *Encyclopedia of Marine Mammals*, (pp. 62–72). San Diego, California: Academic Press.

Beekmans, B. W. P. M., Forcada, J., Murphy, E. J., De Baar, H. J. W., Bathmann, U. V., & Fleming, A. H. (2010). Generalised additive models to investigate environmental drivers of Antarctic minke whale (*Balaenoptera bonaerensis*) spatial density in austral summer. *Journal of Cetacean Research and Management*, *11*(2), 115–129.

Bernstein, E. R., Geiger, C. a., DeLiberty, T. L., & Lemcke-Stampone, M. D. (2015). Antarctic sea-ice thickness and volume estimates from ice charts between 1995 and 1998. *Annals of Glaciology*, *56*(69), 383–393.

Bombosch, A., Zitterbart, D. P., Van Opzeeland, I., Frickenhaus, S., Burkhardt, E., Wisz, M. S., & Boebel, O. (2014). Predictive habitat modelling of humpback (*Megaptera novaeangliae*) and Antarctic minke (*Balaenoptera bonaerensis*) whales in the Southern Ocean as a planning tool for seismic surveys. *Deep Sea Research Part I: Oceanographic Research Papers*, *91*, 101–114.

Branch, T. (2006). Abundance estimates for Antarctic minke whales from three completed circumpolar sets of surveys, 1978/79 to 2003/04. *Journal for Cetacean Research and Management*, *SC/58/IA18*(1), 1–28.

Brierley, A. S., Fernandes, P. G., Brandon, M. a., Armstrong, F., Millard, N. W., McPhail, S. D., Stevenson, P., Pebody, M., Perrett, J., Squires, M., Bone, D. G., & Griffiths, G. (2002). Antarctic krill under sea ice: elevated abundance in a narrow band just south of ice edge. *Science*, *295*(5561), 1890–1892.

Brodie, P. F. (2001). Feeding mechanics of rorquals (*Balaenoptera* sp.). In *Secondary Adaptations of Tetrapods to Life in Water*, (pp. 345–352). Munich, Germany: Verlag.

Cavalieri, D. J. (2003). 30-Year satellite record reveals contrasting Arctic and Antarctic decadal sea ice variability. *Geophysical Research Letters*, *30*(18), 4–7.

Cavalieri, D. J., Crawford, J., Drinkwater, M., Emery, W. J., Eppler, D. T., Farmer, L. D., Goodberlet, M., Jentz, R., Milman, A., Morris, C., Onstott, R., Schweiger, A., Shuchman, R., Steffen, K., Swift, C. T., Wackerman, C., & Weaver., R. L. (1992). NASA Sea Ice Validation Program for the Defense Meterological Satellite Program Special Sencor Microwave Imager: Final Report. *NASA Technical Memorandum*, *104559*, 126 pages.

Cavalieri, D. J., & Parkinson, C. L. (2008). Antarctic sea ice variability and trends, 1979–2006. *Journal of Geophysical Research*, *113*(C7), 1–19.

Da Rocha, J. M., & Braga, N. M. A. (1982). Brazil Progress Report on cetacean research, June 1980 to May 1981. *Reports of the International Whaling Commission*, (32), 155–159.

Dedrick, K. R., Partington, K., Van Woert, M., Bertoia, C. A., & Benner, D. (2001). U.S. National/Naval Ice Center Digital Sea Ice Data and Climatology. *Canadian Journal of Remote Sensing*, *27*(5), 457–475.

DeLiberty, T. L., Geiger, C. A., Ackley, S. F., Worby, A. P., & Van Woert, M. L. (2011). Estimating the annual cycle of sea-ice thickness and volume in the Ross Sea. *Deep-Sea Research Part II: Topical Studies in Oceanography*, *58*(9-10), 1250–1260.

Ensor, P. H. (1989). Minke whales in the pack ice zone, East Antarctica, during the period of maximum annual ice extent. *Reports of the International Whaling Commission*, *39*, 219–225.

ESRI (2015). *ArcGIS geographic information system version 10.3.1*. Environmental Systems Research Institute, Redlands, CA.

Fahrbach, E., Rohardt, G., Scheele, N., Schroder, M., Strass, V., & Wisotzki, A. (1995). Formation and discharge of deep and bottom water in the northwestern Weddell Sea. *Journal of Marine Research*, *53*(4), 515–538.

Friedlaender, A. S., Goldbogen, J. A., Nowacek, D. P., Read, A. J., Johnston, D., & Gales, N. (2014). Feeding rates and under-ice foraging strategies of the smallest lunge filter feeder, the Antarctic minke whale (*Balaenoptera bonaerensis*). *Journal of Experimental Biology*, *217*(16), 2851–2854.

Friedlaender, A. S., Halpin, P. N., Qian, S. S., Lawson, G. L., Wiebe, P. H., Thiele, D., & Read, A. J. (2006). Whale distribution in relation to prey abundance and oceanographic processes in shelf waters of the Western Antarctic Peninsula. *Marine Ecology Progress Series*, *317*, 297–310.

Friedlaender, A. S., Johnston, D. W., Fraser, W. R., Burns, J., Patrick N., H., & Costa, D. P. (2011). Ecological niche modeling of sympatric krill predators around Marguerite Bay, Western Antarctic Peninsula. *Deep-Sea Research Part II: Topical Studies in Oceanography*, *58*(13-16), 1729–1740.
URL http://dx.doi.org/10.1016/j.dsr2.2010.11.018

Friedlaender, A. S., Lawson, G. L., & Halpin, P. N. (2009). Evidence of resource partitioning between humpback and minke whales around the western Antarctic Peninsula. *Marine Mammal Science*, *25*(2), 402–415.

Gales, N. J., Double, M. C., Robinson, S., Jenner, C. K. S., Jenner, M. N., King, E., Gedamke, J., Paton, D., & Raymond, B. (2009). Satellite tracking of southbound East Australian humpback whales (*Megaptera novaeangliae*): Challenging the feast or famine model for migrating whales. *The Scientific Committee of the International Whaling Commission*, (SC61/SH17), 1–12.

Gales, N. J., Kasuya, T., Clapham, P. J., & Brownell, R. L. (2005). Japan's whaling plan under scrutiny. *Nature*, *435*(7044), 883–884.

Gille, S. T. (2002). Warming of the Southern Ocean since the 1950s. *Science*, *295*, 1275–1277.

Goldbogen, J. A., Calambokidis, J., Croll, D. A., Mckenna, M. F., Oleson, E., Potvin, J., Pyenson, N. D., Schorr, G., Shadwick, R. E., & Tershy, B. R. (2012). Scaling of lunge-feeding performance in rorqual whales: Mass-specific energy expenditure increases with body size and progressively limits diving capacity. *Functional Ecology*, *26*(1), 216–226.

Heywood, K. J., Schmidtko, S., Heuzé, C., Kaiser, J., Jickells, T. D., Queste, B. Y., Stevens, D. P., Wadley, M., Thompson, F., Andrew, Fielding, S., Guihen, D., Creed, E., Ridley, J. K., & Smith, W. (2014). Ocean processes at the Antarctic continental slope. *Philosophical Transactions of the Royal Society A*, *372*(2019).

Horwood, J. (1990). *Biology and Exploitation of the Minke Whale*. Boca Raton, Florida: CRC Press.

International Whaling Commission (IWC) (2001). Report of the Scientific Committee. *Journal of Cetacean Research and Management*, *3*.

International Whaling Commission (IWC) (2002). Whale Population Estimates. URL https://iwc.int/Estimate.htm

Izadi, E. (2016). A Japanese fleet killed 333 whales for 'research'. *The Washington Post*.
URL https://www.washingtonpost.com/news/speaking-of-science/wp/2016/03/24/a-japanese-fleet-killed-333-whales-for-research/

Jonsen, I., Bestley, S., Wotherspoon, S., & Summer, M. (2014). Bayesian State-Space Models for Animal Movement.
URL https://cran.r-project.org/web/packages/bsam/bsam.pdf

Kasamatsu, F., Ensor, P., Joyce, G. G., & Kimura, N. (2000). Distribution of minke whales in the Bellingshausen and Amundsen Seas (60W-120W), with special reference to environmental/physiographic variables. *Fisheries Oceanography*, *9*(3), 214–223.

Kranstauber, B., & Smolla, M. (2016). move: Visualizing and Analyzing Animal Track Data.
URL https://cran.r-project.org/package=move

Laws, R. M. (1977). Seals and Whales of the Southern Ocean. *Philosophical Transactions of the Royal Society B: Biological Sciences*, *279*(963), 81–96.

Miyashita, T., Kato, H., & Kasuya, T. (1995). Worldwide map of cetacean distribution based on Japanese sighting data. *National Research Institute of Far Seas Fisheries*.

Murase, H., Kitakado, T., Hakamada, T., Matsuoka, K., Nishiwaki, S., & Naganobu, M. (2013). Spatial distribution of Antarctic minke whales (*Balaenoptera bonaerensis*) in relation to spatial distributions of krill in the Ross Sea, Antarctica. *Fisheries Oceanography*, *22*(3), 154–173.

Nebel, S. (2010). Animal Migration. *Nature Education Knowledge*, *3*(10), 77.

Nicol, S. (2006). Krill, currents, and sea ice: *Euphausia superba* and its changing environment. *BioScience*, *56*(2), 111–120.

Nicol, S., Pauly, T., Bindoff, N. L., Wright, S., Thiele, D., Hosie, G. W., Strutton, P. G., & Woehler, E. (2000). Ocean circulation off east Antarctica affects ecosystem structure and sea-ice extent. *Nature*, *406*(6795), 504–507.

Normille, D. (2015). Scientists renew objections to Japan's whaling program. *ScienceInsider*. URL http://www.sciencemag.org/news/2015/06/scientists-renew-objections-japan-s-whaling-program

Perrin, W. F., & Brownell, R. L. (2002). Minke Whales *Balaenoptera acutorostrata* and *B. bonaerensis*. In *Encyclopedia of Marine Mammals*. San Diego, California: Academic Press.

Pitman, R. L., & Durban, J. W. (2012). Cooperative hunting behavior, prey selectivity and prey handling by pack ice killer whales (*Orcinus orca*), type B, in Antarctic Peninsula waters. *Marine Mammal Science*, *28*(1), 16–36.

Polanowski, A. M., Robbins, J., Chandler, D., & Jarman, S. N. (2014). Epigenetic estimation of age in humpback whales. *Molecular Ecology Resources*, *14*(5), 976–987.

Postlethwaite, C. M., Brown, P., & Dennis, T. E. (2013). A new multi-scale measure for analysing animal movement data. *Journal of Theoretical Biology*, *317*, 175–185.

Potvin, J., Goldbogen, J. A., & Shadwick, R. E. (2010). Scaling of lunge feeding in rorqual whales: An integrated model of engulfment duration. *Journal of Theoretical Biology*, *267*(3), 437–453.

R Development Core Team (2016). *R: A Language and Environment for Statistical Computing*. R Foundation for Statistical Computing, Vienna, Austria.

Ribic, C. A., Ainley, D. G., & Fraser, W. R. (1991). Habitat selection by marine mammals in the marginal ice-zone. *Antarctic Science*, *3*(2), 181–186.

Scheidat, M., Friedlaender, A., Kock, K. H., Lehnert, L., Boebel, O., Roberts, J., & Williams, R. (2011). Cetacean surveys in the Southern Ocean using icebreaker-supported helicopters. *Polar Biology*, *34*(10), 1513–1522.

Smith, R. C., Martinson, D. G., Stammerjohn, S. E., Iannuzzi, R. A., & Ireson, K. (2008). Bellingshausen and western Antarctic Peninsula region: Pigment biomass and sea-ice spatial/temporal distributions and interannual variabilty. *Deep-Sea Research Part II: Topical Studies in Oceanography*, *55*(18-19), 1949–1963.

Stammerjohn, S. E. (2003). Ice-atmosphere interactions during sea-ice advance and retreat in the western Antarctic Peninsula region. *Journal of Geophysical Research*, *108*(C10).

Stammerjohn, S. E., Martinson, D. G., Smith, R. C., & Iannuzzi, R. A. (2008a). Sea ice in the western Antarctic Peninsula region: Spatio-temporal variability from ecological and climate change perspectives. *Deep-Sea Research Part II: Topical Studies in Oceanography*, *55*(18-19), 2041–2058.

Stammerjohn, S. E., Martinson, D. G., Smith, R. C., Yuan, X., & Rind, D. (2008b). Trends in Antarctic annual sea ice retreat and advance and their relation to El Niño-Southern Oscillation and Southern Annular Mode variability. *Journal of Geophysical Research*, *113*(C3).

Tonnessen, J. N., & Johnsen, A. O. (1982). *The History of Modern Whaling*. University of California Press.

Turner, J., Colwell, S. R., Marshall, G. J., Lachlan-Cope, T. a., Carleton, A. M., Jones, P. D., Lagun, V., Reid, P. a., & Iagovkina, S. (2005). Antarctic climate change during the last 50 years. *International Journal of Climatology*, *25*(3), 279–294.

Tynan, C. T., Ainley, D. G., & Stirling, I. (2009). Sea ice: A critical habitat for polar marine mammals and birds. In D. N. Thomas, & G. S. Dieckmann (Eds.) *Sea Ice*. Oxford: Wiley-Blackwell, 2nd ed.

van den Broeke, M. R. (2000). The semi-annual oscillation and Antarctic climate. Part 4: A note on sea ice cover in the Amundsen and Bellingshausen Seas. *International Journal of Climatology*, *20*, 455–462.

Williams, R., Kelly, N., Boebel, O., Friedlaender, a. S., Herr, H., Kock, K.-H., Lehnert, L. S., Maksym, T., Roberts, J., Scheidat, M., Siebert, U., & Brierley, a. S. (2014). Counting whales in a challenging, changing environment. *Scientific reports*, *4*, 4170.

Wood, S., & Scheipl, F. (2014). gamm4: Generalized additive mixed models using mgcv and lme4.
URL https://cran.r-project.org/package=gamm4

World Meteorological Organisation (WMO) (1970). *WMO sea ice nomenclature: Terminology, codes and illustrated glossary*. Secretariat of the World Meteorological Organisation, Geneva.

Zhang, J. (2007). Increasing antarctic sea ice under warming atmospheric and oceanic conditions. *Journal of Climate*, *20*(11), 2515–2529.

Zwally, H. J., Comiso, J. C., Parkinson, C. L., Cavalieri, D. J., & Gloersen, P. (2002). Variability of Antarctic sea ice 1979-1998. *Journal of Geophysical Research*, *107*(C5).

Appendix

GENERALIZED ADDITIVE MODEL RESULTS

The following tables and figures show model results for each generalized additive model performed. Each table provides a summary of the smoothed terms in each model run. Reported statistics include the estimated degrees of freedom (edf) and an F-test to determine if the smoothed function significantly reduces model deviance. Covariates with low edf values represent high variable importance in predicting the MSSI. Each figure panel shows the estimated smooth terms from each run for the three tagged Antarctic minke whales. Figures A.1 and A.2 show the model output for the generalized additive mixed models used for the aggregated whale data, while the following 6 figures are the model outputs from the generalized additive models used for each individual whale.

The solid black line shows the predicted value of the dependent variable with shading representing $\pm$ 2 standard errors. The short, vertical lines along the horizontal axis are the 'rug,' demonstrating the distribution of the observed values. The vertical axis is the estimated smooth function partial response on the scale of the linear predictor variable. It expresses the influence of each dependent variable on the predictor variable, the MSSI, where positive Y values contribute to greater MSSI and negative Y values contribute to MSSI closer to 0, defined here as likely foraging behavior. Results are plotted on the same vertical scale in order to assess the relative influence of each explanatory variable. Dependent variables that demonstrate horizontal responses on the predictor's mean indicate no influence on the MSSI (as seen in Figure A.1.f).

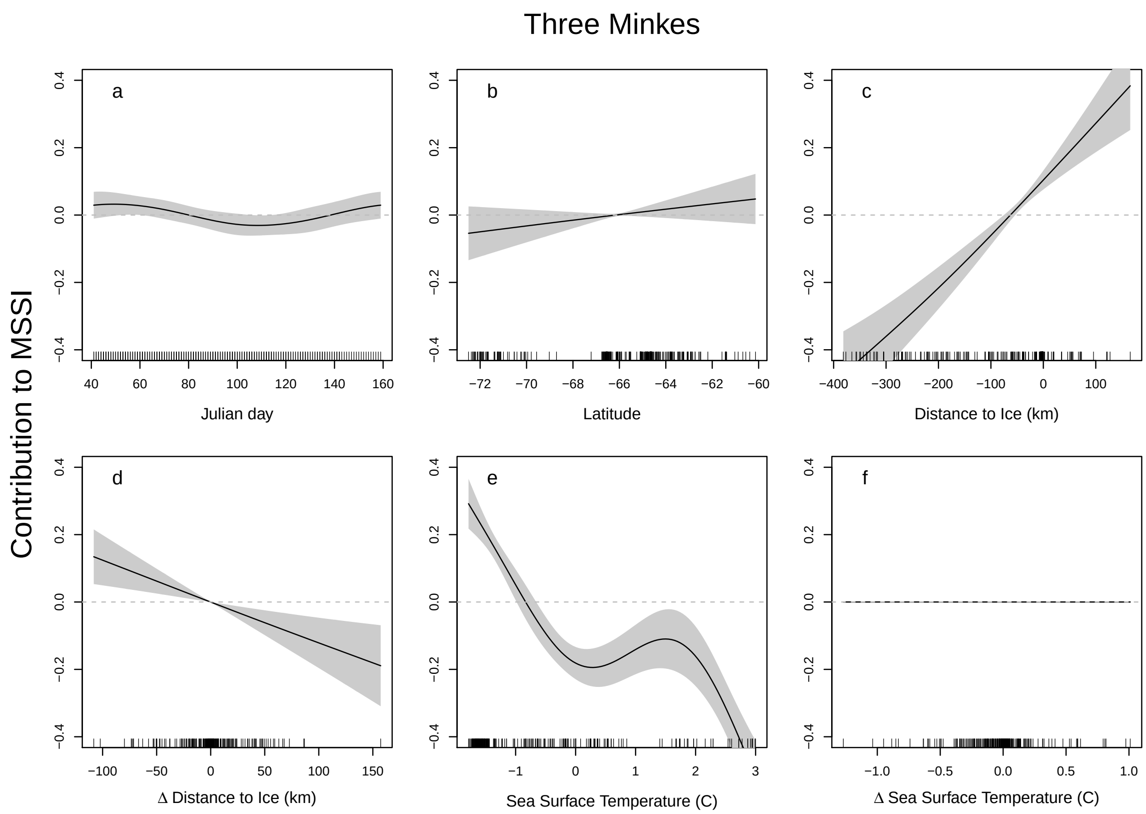

Figure A.1: Smoothed response curves of selected environmental covariates modeling the MSSI in the generalized additive mixed model for the three Antarctic minke whales.

Table A.1: Reported statistics of selected environmental covariates modeling the MSSI in the generalized additive mixed model for the three Antarctic minke whales.

	edf	F	p-value
Julian Day	1.444	30.74	0.0352
Latitude	6.816e-01	8.895	0.0901
SIE	1.501	458.1	6.53e-15
ΔSIE	9.560e-01	88.14	0.0042
SST	3.672	1016	<2e-16
ΔSST	4.663e-08	0	1.000

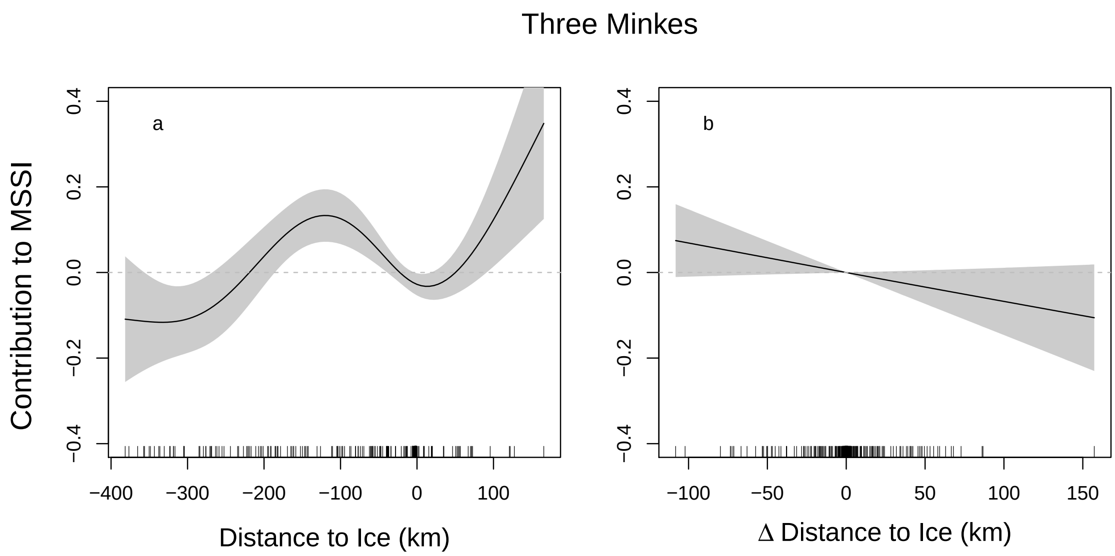

Figure A.2: Smoothed response curves of selected distance to the sea ice extent covariates modeling the MSSI in the generalized additive mixed model for the three Antarctic minke whales.

Table A.2: Reported statistics of selected distance to the sea ice extent covariates modeling the MSSI in the generalized additive mixed model for the three Antarctic minke whales.

	edf	F	p-value
SIE	3.689	147.0	2.44e-05
ΔSIE	0.765	14.27	0.0444

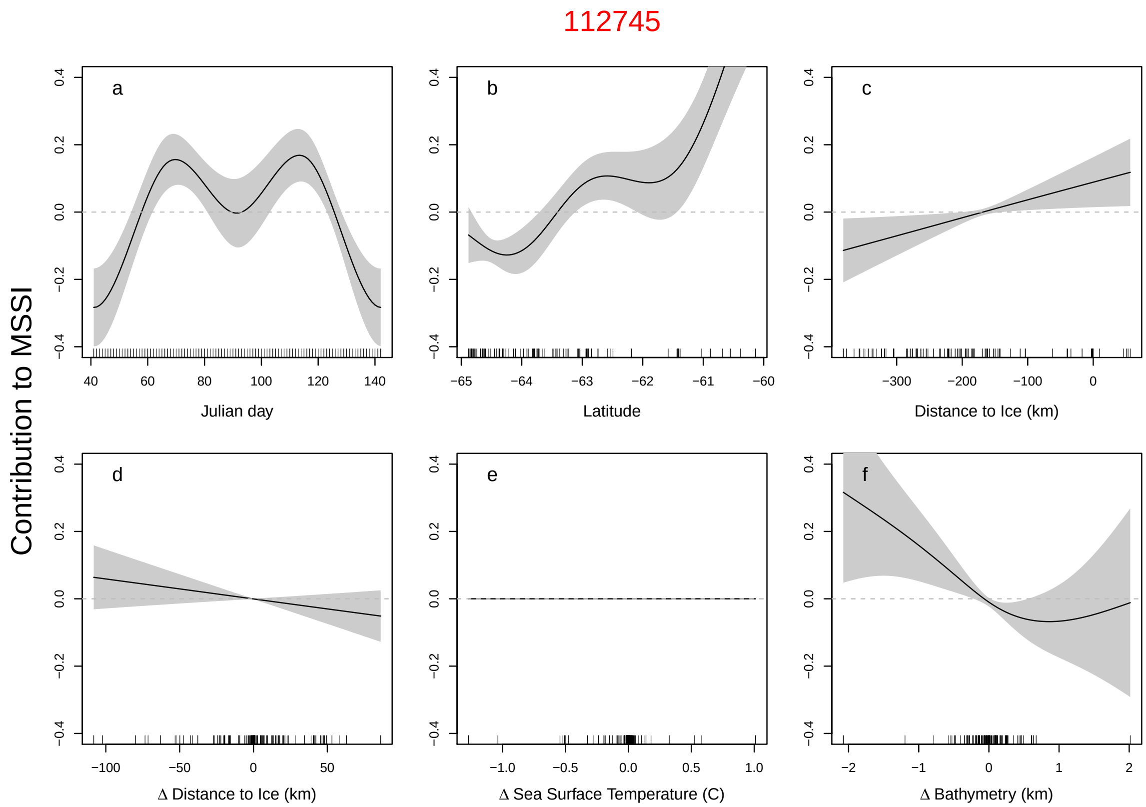

Figure A.3: Smoothed response curves of selected environmental covariates modeling the MSSI in the generalized additive model for whale number 112745.

Table A.3: Reported statistics of selected environmental covariates modeling the MSSI in the generalized additive mixed model for whale number 112745.

	edf	F	p-value
Julian Day	2.952	12.68	1.56e-07
Latitude	3.761	16.10	1.89e-11
SIE	8.295e-01	1.465	0.007
ΔSIE	6.318e-01	0.462	0.0839
ΔSST	1.847e-09	0	0.757
Δbath	2.263	2.596	0.005

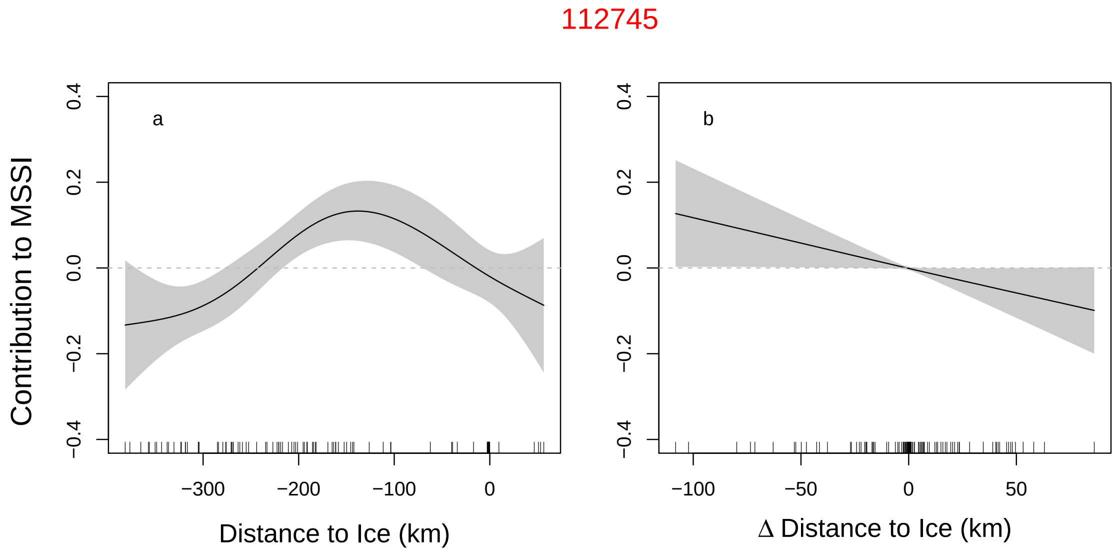

Figure A.4: Smoothed response curves of selected distance to the sea ice extent covariates modeling the MSSI in the generalized additive model for whale number 112745.

Table A.4: Reported statistics of selected distance to the sea ice extent covariates modeling the MSSI in the generalized additive mixed model for whale number 112745.

	edf	F	p-value
SIE	3.082	4.432	0.0005
ΔSIE	0.823	1.058	0.0239

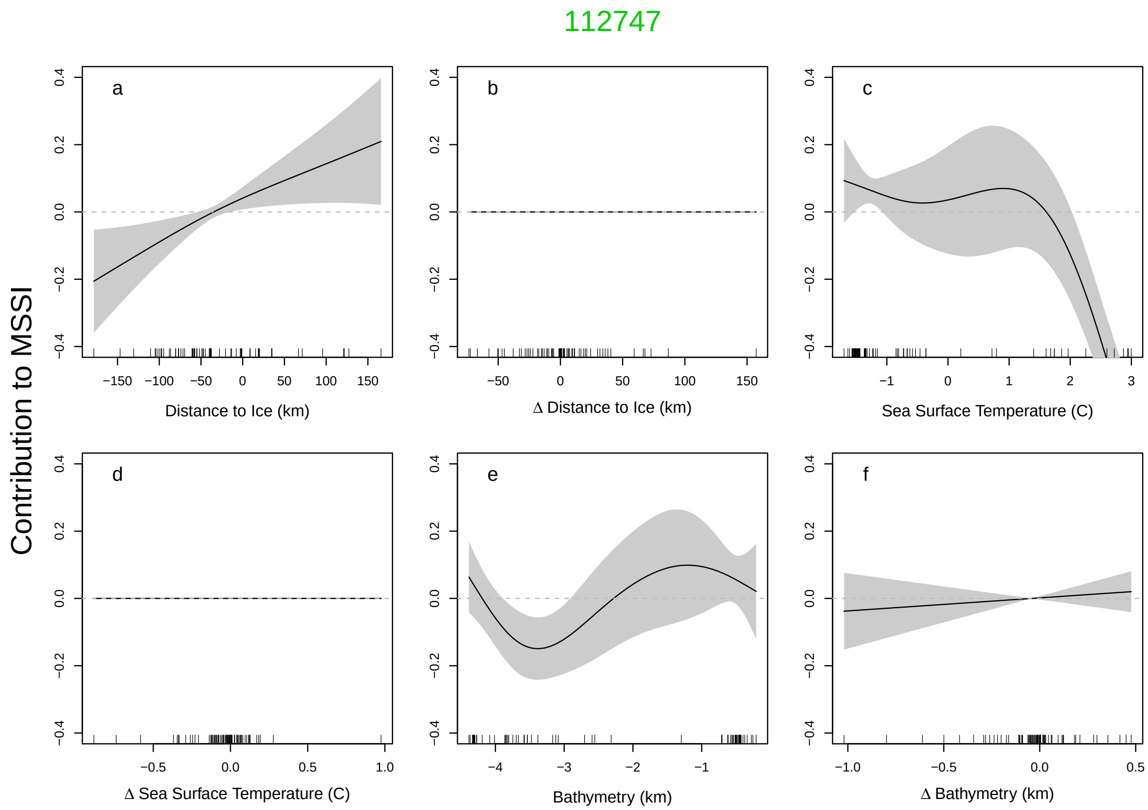

Figure A.5: Smoothed response curves of selected environmental covariates modeling the MSSI in the generalized additive model for whale number 112747.

Table A.5: Reported statistics of selected environmental covariates modeling the MSSI in the generalized additive mixed model for whale number 112747.

	edf	F	p-value
SIE	1.377	2.081	0.0051
ΔSIE	3.557e-09	0	0.5249
SST	3.259	21.22	1.42e-14
ΔSST	8.096e-10	0	0.6473
Bath	3.264	3.314	0.0045
ΔBath	4.084e-01	0.1110	0.2791

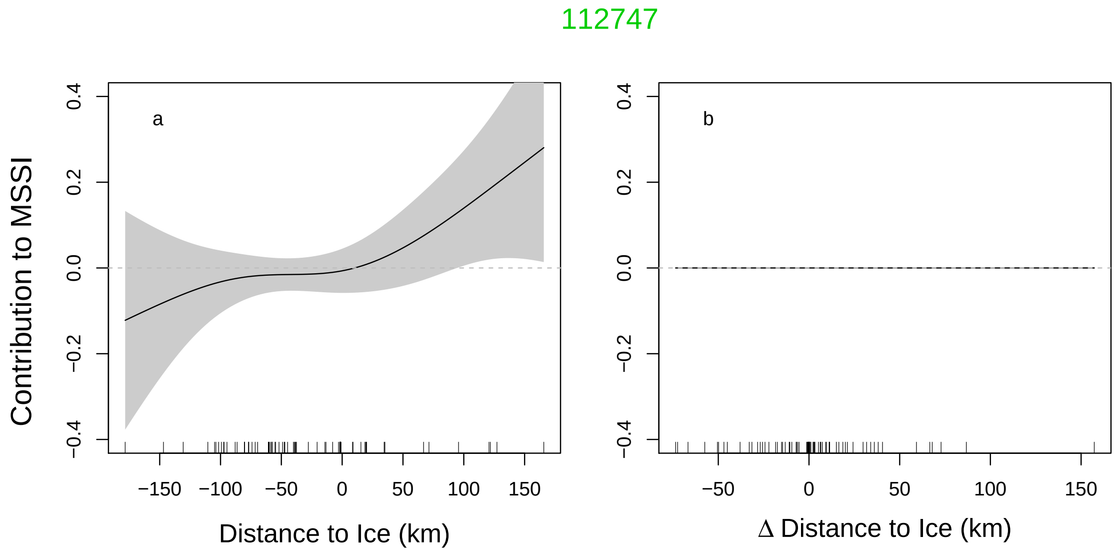

Figure A.6: Smoothed response curves of selected distance to the sea ice extent covariates modeling the MSSI in the generalized additive model for whale number 112747.

Table A.6: Reported statistics of selected distance to the sea ice extent covariates modeling the MSSI in the generalized additive mixed model for whale number 112747.

	edf	F	p-value
SIE	2.239	1.438	0.0629
ΔSIE	1.432e-09	0	0.6657

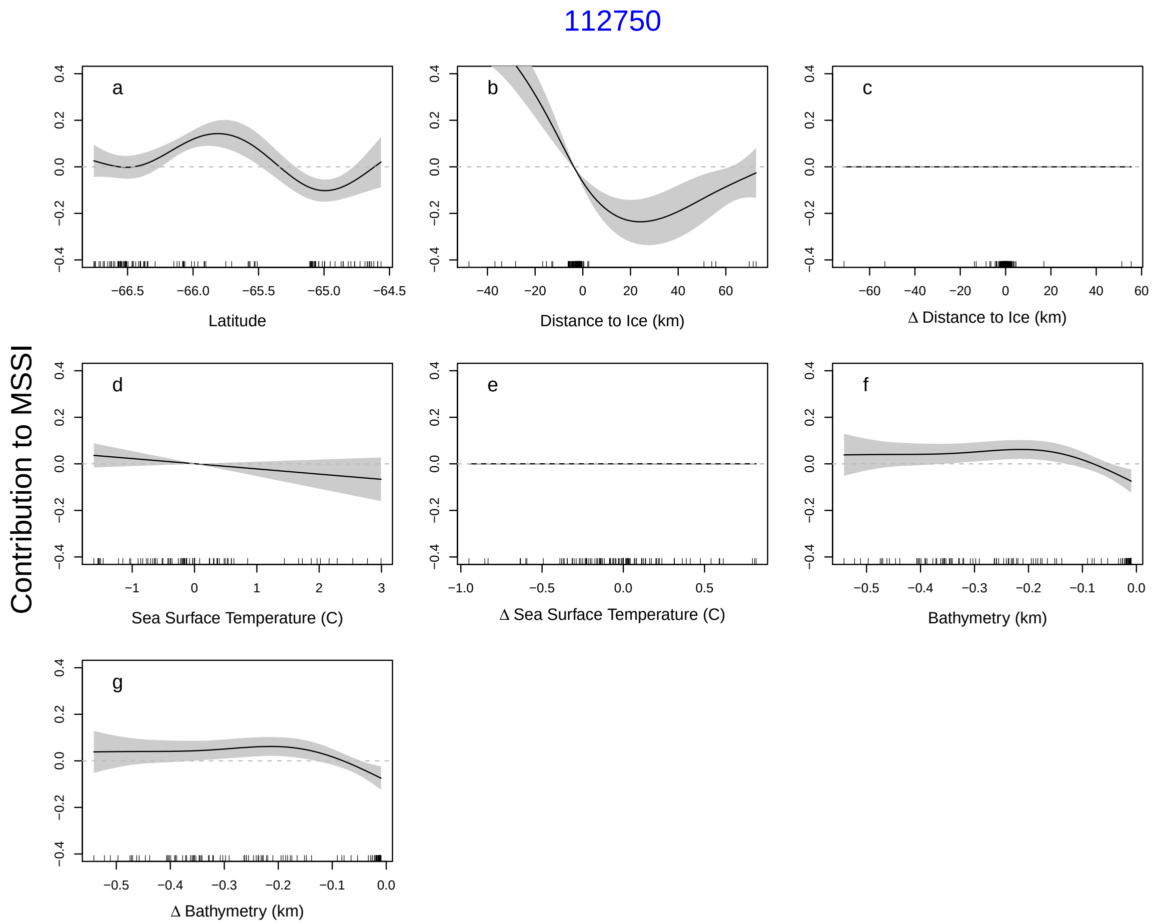

Figure A.7: Smoothed response curves of selected environmental covariates modeling the MSSI in the generalized additive model for whale number 112750.

Table A.7: Reported statistics of selected environmental covariates modeling the MSSI in the generalized additive mixed model for whale number 112750.

	edf	F	p-value
Latitude	3.962	15.66	1.26e-11
SIE	3.545	20.56	4.58e-15
ΔSIE	8.500e-09	0	0.5092
SST	5.754e-01	0.503	0.0564
ΔSST	2.495e-09	0	0.8848
Bath	2.789	2.623	0.0060
ΔBath	3.825e-01	0.245	0.1056

112750

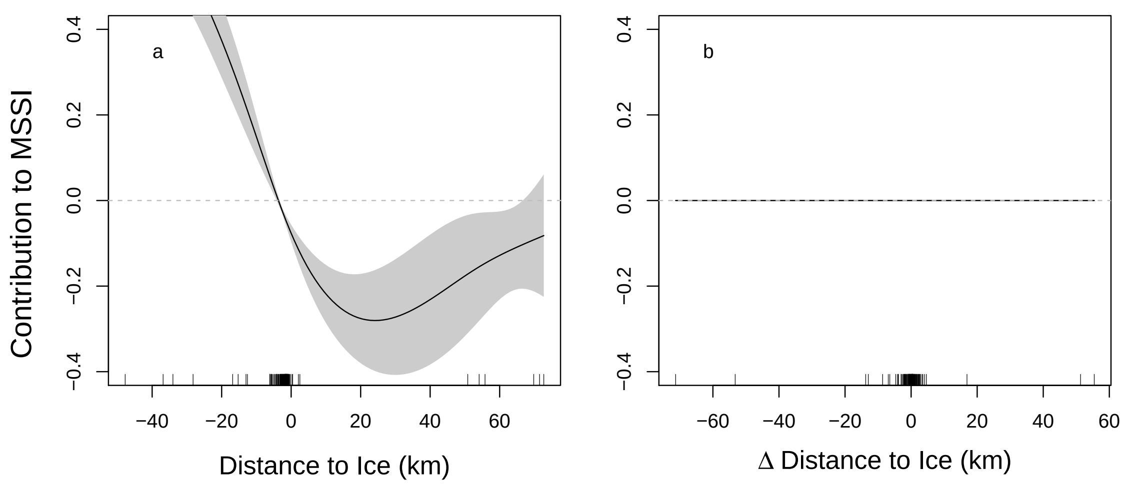

Figure A.8: Smoothed response curves of selected distance to the sea ice extent covariates modeling the MSSI in the generalized additive model for whale number 112750.

Table A.8: Reported statistics of selected distance to the sea ice extent covariates modeling the MSSI in the generalized additive mixed model for whale number 112750.

	edf	F	p-value
SIE	3.642	39.05	<2e-16
ΔSIE	8.446e-09	0	0.423